

1 **The impact of resolving the Rossby radius at mid-latitudes**
2 **in the ocean: results from a high-resolution version of the**
3 **Met Office GC2 coupled model by H. T. Hewitt et al.**
4

Review by Stephen Griffies

We thank Dr. Griffies for his constructive comments and address them here.

This is generally a well written and concise entree into a suite of coupled climate models run for 20 years. To my knowledge the finest resolution model, GC2.1-N512O12, is the state-of-the-science, at least for global models run for more than a few years. This point is worth emphasizing.

- A sentence has been included (p3, line1) to emphasise that with the resolution of atmosphere and ocean components and hourly coupling, this model is state of the art.

The tasks required are immense to produce a sensible simulation, even for the rather brief 20 years considered here. I applaud this effort, though note it is far from complete!

Yet as an introduction to the model suite, this is a useful contribution to the literature, and it provides an important peer-reviewed touchpoint for the developers. This manuscript is appropriate for GMD. I recommend publication after minor revisions.

Others who have developed models of this resolution with refined coupling periods (hourly or smaller) sometimes have problems related to coupled ocean/sea ice instabilities as discussed by Hallberg (CLIVAR Exchanges, No.65 (Vol 19 No.2) July 2014). It would serve the reader to know if you encountered any similar instabilities, and if so, what methods were used to suppress them. If you did not encounter such instabilities, it would be useful to state that as well.

- We did not experience instabilities associated with the hourly coupling. This is stated (p4, lines 24-25)

The Weddell Sea polynya in GC2.1-N512O12 warrants more discussion. In similar models at GFDL, we have seen that such polynyas can increase ACC transport, much as noted on page 10, lines 10-22. Do any of the other models in your suite have a polynya? Is the polynya large in area and going very deep? How long does it last? I am puzzled that the SST biases in

Figures 2 and 3 show no sign of the polynya. In other models I have seen, such polynyas increase SST due to release of mid-depth heat. That SST signature is missing here. Perhaps the polynya is only for a year or two, and is averaged out by the 10 year mean? Please discuss, as this is an important feature to expose.

- Further investigation shows that the polynya first appears in year 12 and varies from year-to-year. In years without a polynya, the maximum mixed layer depth is less than 1000m. However, in year 15, the maximum mixed layer depth is 1556 m and in year 20 it is 2070m. More information about the polynya and its variability is given on p8, line 7, p10, lines 6-10 and in the new figure 9.

Pg1, line18: I appreciate that it is the surface ocean that the atmosphere cares about, and the sentence is referring to air-sea fluxes. But the sentence can be construed, incorrectly, to mean that ONLY surface eddies and boundary currents are necessary to do air-sea coupling right. As the authors show in this paper, there is more to air-sea fluxes than the surface ocean. For example, overflows and the AMOC are key. So I recommend finding a different way to write this sentence.

- Sentence has been changed in abstract (p1, line 17-18)

Pg1,line23: Admittedly a picky point, but worth being precise: hours are listed here as "frequency" for coupling (1-hour versus 3-hour). In fact, these are the "coupling periods" not the "coupling frequencies".

- P1, line 23 frequency changed to period (also p4, line 14 and in table 1)

Pg3,line5: Behrens et al. (2013) should be Behrens (2013). This citation refers to a single-authored PhD thesis.

- P3, line 8 reference corrected

Pg4,line9: again, "3-hourly to hourly" refers to "coupling period" not "coupling frequency"

- P4, line 14 corrected to period

Pg4,line11: it is not clear what model is being referred to here when discussing the time step. I assume the ocean, but it should be clearly stated.

- P4, line 16 ocean inserted

Pg4,line27: Viscosity is a positive number. The biharmonic operator carries the negative sign. Please change. Doing so will also make the sentence correct. Namely, it presently reads "a reduction in the bilaplacian viscosity from $-5e11$ to $-0.25e10$ ". With the minus sign, this is

not a reduction, but an increase! Again, just drop the minus signs on the viscosity so that all will make sense.

- P5, line 4 viscosity sign corrected

Pg5,line5: Including tides generally increases the flow speed in simulations. So what you mean here is that there is missing "tidal dissipation" in the model. That is, you are not suffering from missing tides, but instead suffering from missing tidal dissipation.

- P5, line 15 tides changed to tidal dissipation

Pg5,line6: what is "atmospheric theta"? Please define the jargon.

- P5, line 17 theta changed to temperature.

Pg5,line28: what sort of "instabilities" do you find enhanced with the finer atmosphere? Those instabilities discussed earlier near the UK due to missing tidal dissipation? Something else?

- P6, lines 7- 8 clarification added to the instabilities

Pg8,lines10-11: More heat into the ocean interior is NOT what Griffies et al (2015) found with the GFDL CM2.6 simulation (1/10th degree ocean) relative to the coarser ocean (1/4th degree) in CM2.5. Instead, enhanced mesoscale eddy activity led to less heat entering the ocean. So...why does GC2.1-N512012 get warmer in the interior than GC2-N512? Could it be an increase in spurious diapycnal diffusion from advection errors? It is useful to speculate here, even if you do not perform a budget analysis as in Griffies et al.

- Paragraph has been inserted p8, lines 26-32 to discuss the heat uptake issue and contrast with Griffies et al. (2015)

Pg9, It is useful to state how the mixed layer depth is computed.

- This has been added to a footnote on p9

Pg 10,line6: a more recent Denmark St overflow measurement paper is Jochumsen et al. (2012), 10.1029/2012JC008244

- P11, line 4 Jochumsen reference added

pg10,line18: a more recent Drake Passage transport paper is Meredith et al. (2011) 10.1029/2010RG000348

- P11, line 13 Meredith reference added

*Pg10, equation (1): dS is not defined. I presume it is $dS = dx * dz$. Please specify.*

- P12, lines 4-6 definition of dS and also dA added

pg10,line31: A_iso is not the "isopycnal diffusion". Instead, it is the "isopycnal diffusivity". Or more properly, it is the "isoneutral diffusivity", which is consistent with terminology used elsewhere in this manuscript.

- P12 line 3 changed to isoneutral diffusivity and on p14, lines 25-26

pg11, line1-3: I puzzled by this discussion. You state that the isoneutral fluxes are smaller than other terms, but then state, parenthetically, that the dianeutral diffusive fluxes are very small when integrated over the full depth. I think there is some confusion here. In particular, the dianeutral diffusive fluxes, which are computed as vertical diffusion in NEMO, should have a zero depth integral since vertical diffusion only redistributes heat within a column. In contrast, the depth integrated isoneutral diffusion fluxes have a nonzero depth integral. Are you arguing that the depth integrated isoneutral diffusive heat fluxes are small?

- P12 line 7 This comment is correct. The wording has changed to isoneutral

pg11, lines23-24: I fail to see how removing a global mean from the right hand side of equation (1) will not be seen by the left hand side of equation (1). Is that what you want? Please detail more of what you mean by "subtracting the global mean imbalance from the surface fluxes before integrating zonally and meridionally." It is vague as stated.

- Removing the global mean surface flux from the rhs of (1) is equivalent to removing the global integral of the temperature drift from the lhs of (1). This means that the imbalance represents the residual local drifts. Text has been added to make this clear (p12, line 31 – p13, line 4)

pg12, line13-ff: Again, I wonder how much of what you are seeing relates to the Weddell Sea polynya

- A caveat has been added on p13, line 31-p14, line 1

pg13,line32: GFDL prediction folks claim that eddying oceans are too expensive for initialization schemes. So they are not pursuing ocean resolution. That contrasts with your motivation at the Met Office. The community would be well served to know more about your initialization strategies with an eddying ocean. It is worth at least a paragraph.

- A short paragraph on initialisation has been included on p15 lines 26- p16, line 2

Figure 1: legend font is tiny; needs to be larger.

- Figure 1: legend size increased

Figures 2,3,4: is the land/sea mask based on the model grid, or based on an observed topography dataset? It looks like observed. I suggest it more useful and honest for a modelling paper to show the land/sea mask based on the model grid. I also dislike white land since there is also a white part of the colour bar for ocean fields. I suggest colouring the land light brown or light gray, in order to clearly distinguish water from land.

- Figures 2,3,4: land has been changed to grey and mask from model grid used

Figure 3: the colour range should be smaller in order to better see the anomalies.

- Figure 3: range reduced to -2 to 2

Figure 5: the HadISST values should be coloured to better distinguish from the many model lines. The present light gray shading does not come through well.

- Figure 5: HadISST values coloured. Legend changed to GC2.1-N512O12

Figure 6: how deep does the MLD penetrate in the saturated regions? This issue goes to the question about how significant is the polynya.

- Figure 6: Maximum MLD in the average is 788m. However, as seen in the extra figure, the polynya only appears in the last 9 years of the simulation and then it is only in the final year that it extends down to below 2000m. Land has been changed to grey and definition of sea ice edge added to caption.

Figure 9: The bottom topography appears nearly the same across the ocean resolutions. Are you sure you are showing the proper bottom? Does the model make use of the partial bottom cells? If so, then the bottom shown here does not appear to reflect the partial cells; this instead figure looks like it is showing full cells. Again, it is preferable to show the what the model is actually using.

Figure 9 (now figure 10): The model does use partial cells and the average topography is changing between ORCA025 and ORCA12

Review by Andy Hogg

We thank Dr Hogg for his constructive comments and address them here.

This manuscript describes the development of a version of the UKMO GC2 coupled climate model with enhanced resolution in both atmosphere and ocean, as well increased coupling frequency. The development of this model is a significant achievement – and at 1/12 ocean resolution is, to my knowledge the highest resolution coupled model available. In addition, and contrary to many previous coupled models with high ocean resolution, the authors systematically include the effect of enhanced atmospheric resolution.

However, the technical achievements outlined here are not quite matched by the depth of analysis of the model results. In many cases, changes between results from different simulations are causally attributed with only a superficial analysis. I accept that, for GMD readers, the attribution of different physical effects may be of secondary importance to the technical achievement; but if the authors want to imply causality then a more rigorous analysis is required. In a number of cases (details below) the authors could sidestep this issue by rephrasing the text - i.e., by making it clear that they are speculating on the cause rather than attributing, and pointing out where additional experiments will enable them to resolve the uncertainty. If these issues are addressed I would be happy to recommend this paper as a suitable contribution to GMD.

We have made a number of revisions which we hope address the comments.

On p.4 (line 26) it is noted that the transition from ORCA025 to ORCA12 is accompanied by a reduction in the isoneutral diffusivity from 300 to 125 m²/s. It would help to have a justification of this change - in particular, if eddies are fully resolved, why do we need isoneutral diffusivity at all? If it is needed, then on what basis do we choose 125?

This question is relevant because, for example, the reduction in SST biases is attributed to resolution (p. 6, line 24). However, this result (at least for the Southern Ocean warm bias) might alternatively be attributed to reduced parameterised upwards eddy heat flux. This effect may be consistent with the analysis on p.11, which shows a reduction in the time-mean southward heat transport at southern latitudes. And, finally, in the discussion there is reference to previous experiments in which changes in isoneutral diffusivity are associated with high-latitude cooling, but the authors argue that this “is believed to be a secondary effect” due to the long timescales associated with that paper. This is one example where the

authors need to pose one of two possible causes (with further experiments to tease out the root cause) or else perform a more in-depth analysis. For this case there are some clear, but simple, tests which could be performed. The isoneutral diffusivity contribution to the southward (or upwards) heat flux could be calculated explicitly. Alternatively, this question could be resolved by one additional GC2.1 simulation with reduced isoneutral diffusivity.

- We agree that the isoneutral diffusivity needs more discussion.
- We include the following text on p5, lines 7-11 ‘While reducing the isoneutral tracer diffusivity is consistent with the increase in resolution, we note that results may have some sensitivity to its magnitude. Experiments to investigate the impact of this parameter in GC2 were not performed but will be pursued in future work with GC3 (the next version of the coupled model).’
- In the discussion, the following text has been included on p14, lines 28-32 ‘Given that the results here exhibit some consistency with those of Pradal and Gnanadesikan (2014) in the Southern Ocean, further work is required to quantify the role of isoneutral diffusivity in producing changes in SST on decadal timescales.’

I wasn't entirely convinced by the description of the MOC changes (bottom of p. 9). Firstly, it is argued that changes are dominated by the cell associated with NADW - this may be true, but the other cells are not shown. This manuscript would be much more complete if the full MOC were shown, including the Southern Ocean (which would require transforming the overturning analysis into density space). In addition, the attribution of both NADW formation and Denmark Strait outflow increases to higher resolution seems fraught; the GC2.1 case sees a modest increase in both of these quantities, implying that the higher coupling frequency is partly response for the changes.

- Unfortunately, we did not have 5 day means of the full velocity field saved to allow calculation of the overturning in density space. As many authors have shown, this field is not entirely meaningful unless the eddy component is included. Calculations of the overturning in density space with monthly means suggest that the changes in NADW due to resolution and coupling period are robust but we can't be certain about the AABW cell. The 5 day mean velocity fields was an oversight in setting up the model diagnostics and we will address this issue in future runs with the GC3 model for CMIP6. A comment has been added to the paper on this point (p10, lines 28-30).
- We have however modified the text on p10, lines 21-26 to reflect that the coupling frequency plays a role as well as on p11, line 6 and p14, lines 12-13

On p.10, l. 17, the ACC transport increase at higher resolution is noted as being consistent with both enhanced NADW and the Weddell Sea polynya. It seems unlikely that NADW formation can affect ACC transport in a short 20 year run (see Allison et al., JMR, 2011) - meaning that it is most likely that the Weddell Sea effect is dominating. Either way, both effects probably need to be supported in the form of a reference to existing literature. On a similar note, it seems likely that the small ACC transport in these simulations may be linked to weak AABW formation because of the Southern Ocean SST bias. This point could be further clarified if the full MOC were shown as suggested above.

- P11, lines 20-23 we have included a reference to Jones et al. (2011) who show that transient responses in the ACC can be seen within 10 years in their idealised experiments.
- References have been added for the NADW and the Weddell Sea links to the ACC (p11, lines 17-18)

The paragraph starting on p. 12, l. 29, is somewhat unconvincing. The case is made that refining both atmosphere and ocean resolution is important to gain the full benefit of resolution improvements. Yet, for almost all the metrics shown here, the N512 case showed only minor differences from GC2 (as noted in the first paragraph in this section). It may be that there are other metrics on which the N512 case performs well, but they are not shown here, so should not be included in the summary of this paper.

- The paragraph p15, lines 11-17 has been changed in response to the comments to state that ocean resolution and coupling frequency is important and states that further work is required to quantify whether a high resolution atmosphere component is required.

p. 4, line 22: I'm not sure I would call this an aspect ratio. Maybe just ratio?

- P4, line 29 aspect deleted

p. 6, line 9: It seems to me that the Southern Ocean SST biases here are larger than they were for CMIP-5. If true, then this should be explicitly stated, along with a reference to the published bias (it looks as if you're hiding something by stressing the pattern, rather than magnitude, of the bias).

- Comments on the magnitude of SST biases in GC2 have been added on p6 lines 21-25. Basically the SST warmed everywhere in GC2 relative to the CMIP5 model HadGEM2-AO (see figure 1 of Williams et al., 2015) leading to improvements in the Northern hemisphere and degradations in the Southern hemisphere.

Several times through the manuscript the N512O12 simulation is listed as N512-ORCA12 - best to be consistent if possible. (p. 6, l.24; p. 7, l.24; legend of Fig. 5)

- Corrected to GC2.1-N512O12 in text and figures 5, 7, 8, 11, 12

p.10, l.31: isopycnal -> isopycnal

- Changed isopycnal to isoneutral p12, line 3

p. 11, l.4: There are four instances of “change/s” in the one sentence here, which becomes a little repetitive.

- Text on p12, lines 18-22 changed to improve reading

p. 12, l.17: I'm not convinced that we expect more slumping of ACC isopycnals in the eddy-resolving simulation - changes in eddy KE are more likely to control the ACC through enhanced vertical momentum transport - but if there is a previously published expectation supporting this statement then I suggest a reference.

- Text has been changed on p13, lines 27- p14, line 1 to reflect the discussion on the ACC

The reference to “seamless” prediction makes little sense to those outside the UKMO community, and I suggest it should be either explained to great depth, or removed.

- P15, line 18 seamless removed

p. 35, l.6: specify “north pole”.

- P49. North Pole specified

The impact of resolving the Rossby radius at mid-latitudes in the ocean: results from a high-resolution version of the Met Office GC2 coupled model

Helene T. Hewitt¹, Malcolm J. Roberts¹, Pat Hyder¹, Tim Graham¹, Jamie Rae¹, Stephen E. Belcher¹, Romain Bourdallé-Badie⁴, Dan Copsey¹, Andrew Coward², Catherine Guiavarch¹, Chris Harris¹, Richard Hill¹, Joël J.-M. Hirschi², Gurvan Madec^{2,3}, Matthew S. Mizielinski¹, Erica Neining¹, Adrian L. New², Jean-Christophe Rioual¹, Bablu Sinha², David Storkey¹, Ann Shelly¹, Livia Thorpe¹, and Richard A. Wood¹

[1]{Met Office, Exeter, United Kingdom}

[2]{National Oceanography Centre, Southampton, United Kingdom}

[3]{IPSL, Paris, France}

[4]{Mercator Océan, Toulouse, France}

Correspondence to: H. T. Hewitt (helene.hewitt@metoffice.gov.uk)

Abstract

There is mounting evidence that resolving mesoscale eddies and western boundary currents ~~in the surface ocean field as well as topographically-controlled flows~~ can play an important role in air-sea interaction associated with vertical and lateral transports of heat and salt. Here we describe the development of the Met Office Global Coupled Model version 2 (GC2) with increased resolution relative to the standard model: the ocean resolution is increased from $1/4^\circ$ to $1/12^\circ$ (28km to 9km at the Equator), the atmosphere resolution increased from 60km (N216) to 25km (N512) and the coupling ~~period frequency increases~~ reduced from 3-hourly to hourly. The technical developments that were required to build a version of the model at higher resolution are described as well as results from a 20 year simulation. The results demonstrate the key role played by the enhanced resolution of the ocean model: reduced Sea Surface Temperature biases, improved ocean heat transports, deeper and stronger overturning circulation and a stronger Antarctic Circumpolar Current. Our results suggest that the

1 improvements seen here require high resolution in both atmosphere and ocean components as
2 well as high frequency coupling. These results add to the body of evidence suggesting that
3 ocean resolution is an important consideration when developing coupled models for weather
4 and climate applications.

5

6 **1 Introduction**

7 On the scale of the Rossby radius, the ocean is rich with mesoscale eddies (Chelton et al.,
8 2011) and oceanic fronts. There is mounting evidence from satellite observations that
9 mesoscale features in the Sea Surface Temperature (SST) field can drive comparable
10 variations in atmospheric winds and surface fluxes (Chelton and Xie, 2010; Frenger et al.,
11 2015). While at the basin scale, observed correlations between SST and surface winds are
12 negatively correlated, indicating that the atmosphere is driving the ocean, in frontal regions
13 with high mesoscale activity, such as those associated with Western boundary currents, SST
14 and surface winds are positively correlated, implying that the ocean is driving the atmosphere
15 (Bryan et al., 2010). While the primary response to SST takes place in the atmospheric
16 boundary layer (Chelton and Xie, 2010), there is also evidence that divergence of surface
17 winds may give rise to vertical motions which may penetrate high into the troposphere
18 affecting storm tracks and clouds (e.g., Minobe et al., 2008; Sheldon and Czaja, 2014). Of
19 particular note is the intense rain band in the North Atlantic that follows the path of the Gulf
20 Stream/North Atlantic Current.

21 The recent CMIP5 ocean models have a horizontal resolution of between 1° and $1/4^\circ$.
22 However, with a resolution of 28km at the Equator down to 6km in the Canadian archipelago
23 (due to the tripolar grid), even $1/4^\circ$ remains insufficient to resolve mesoscale eddies which
24 have a typical scale of 50km in the deep ocean at mid-latitudes (Hallberg, 2013). Several
25 climate modelling groups have now built global coupled models with an “eddy resolving”
26 component (e.g., McClean et al., 2011; Bryan et al., 2010; Delworth et al., 2012; Small et al.,
27 2014; Griffies et al., 2015). In this paper, we describe results from coupling the $1/12^\circ$ ocean
28 model (ORCA12) produced by the Drakkar group (Marzocchi et al., 2015; Deshayes et al.,
29 2013; Treguier et al., 2012) to a 25 km (N512) resolution version of the Met Office Unified
30 Model (MetUM) atmosphere. This is the first version of the HadGEM3/GC series (Hewitt et
31 al., 2011; Williams et al., 2015) to resolve the Rossby radius in the ocean at mid-latitudes
32 (with a resolution of 9km at the Equator down to 2km in the Canadian archipelago) and the

1 first coupled experiment with the NEMO ORCA12 ocean configuration. [The development of](#)
2 [a global coupled model with atmosphere and ocean components of this resolution as well as](#)
3 [hourly coupling is the current state of the art for global climate modelling.](#)

4 Evidence from forced ocean simulations demonstrates that resolution enables a more realistic
5 representation of both eddy kinetic energy (Hurlburt et al., 2009; Griffies et al., 2015), narrow
6 boundary currents (e.g., Marzocchi et al., 2015) and representation of complex topography, in
7 particular the sills which connect ocean basins (e.g., improved overflows in the VIKING
8 model at 1/20° resolution; Behrens ~~et al.~~, 2013). In this paper we investigate how ocean
9 resolution drives large-scale changes not only in the ocean but also in the climate system.
10 Changes in the ocean circulation could be important both for present and future climate; for
11 example, in an ocean-only model with a simple domain, Zhang and Vallis (2013) have shown
12 that the changes in mean circulation due to eddy-resolving resolution can affect the net ocean
13 heat uptake under global warming scenarios.

14 In this paper, the model is described in section 2. Our results (section 3) describe the relative
15 impact of the three changes to the model; ocean resolution, atmosphere resolution and
16 coupling frequency. Finally in section 4 we summarise and discuss the results.

18 **2 Model description**

19 The development of the high resolution coupled climate model is based on the Met Office
20 Global Coupled model version 2 (GC2; Williams et al., 2015). GC2 is comprised of the Met
21 Office Unified Model (MetUM; GA6) atmosphere, the JULES land surface model (Best et al.,
22 2011; GL6), the NEMO ocean model (Madec, 2014; GO5; Megann et al., 2014) and the Los
23 Alamos CICE sea-ice model (Hunke et al., 2010; GSI6; Rae et al., 2015). The standard
24 configuration for GC2 has a 60km resolution atmosphere coupled to 1/4° (28km at the
25 Equator reducing polewards) ocean (N216-ORCA025) with coupling between the
26 components (as described in Hewitt et al., 2011) every three hours. GA6 has 85 vertical levels
27 while GO5 has 75 vertical levels with 1m resolution in the top 10m of the ocean (Megann et
28 al., 2014). Although vertical resolution is not explored here, we include details of the vertical
29 levels in appendix A.

1 In addition to GC2, this paper describes three modified versions of GC2 with increased
2 atmosphere resolution, increased coupling frequency and increased ocean resolution. The
3 different model experiments are described below and summarised in Table 1.

4 GC2 has been run with a high 25km (N512) atmosphere resolution and the standard
5 (ORCA025) resolution ocean and we will refer to this as GC2-N512. The scientific
6 differences between N216 and N512 are minimal, as described in Walters et al. (in prep), and
7 are principally associated with the time step (modified from 15min to 10min) and the
8 resolution of the external boundary conditions such as the orography.

9 To facilitate direct scientific comparison with the 1/12° ORCA12 (9km at the Equator
10 reducing polewards) configuration of NEMO, which was developed using NEMO v3.5 rather
11 than 3.4 (Marzocchi et al., 2015), a modified configuration of GC2, referred to here for
12 convenience as GC2.1 was developed. The key scientific and technical changes made to
13 GC2.1 are:

- 14 • ~~An increase a reduction~~ in the coupling ~~period-frequency~~ from 3-hourly to hourly
- 15 • an upgrade to the non-linear free surface scheme rather than the linear free surface
- 16 • a small reduction in the ocean timestep from 1350s to 1200s (to accommodate hourly
17 coupling)
- 18 • small changes associated with river outflows; outflows prescribed over 15m rather
19 than 10m with an enhanced vertical mixing in the outflow region of $1 \times 10^{-3} \text{ m}^2 \text{ s}^{-1}$ rather
20 than $2 \times 10^{-3} \text{ m}^2 \text{ s}^{-1}$
- 21 • an upgrade of the sea ice model from CICE4 to CICE5 (Hunke et al., 2015). This
22 upgrade was for technical reasons and the science of the sea ice configuration remains
23 unchanged.

24 The reduction of the coupling period in GC2.1 did not lead to coupled ocean/sea ice
25 instabilities as described by Hallberg (2014).

26 To assess the impact of ocean resolution, a traceable GC2.1 configuration with ORCA12 was
27 then built (further technical details and model performance issues are discussed in appendix
28 B). We chose to increase the atmosphere resolution to N512 in order to maintain a similar
29 ~~aspect~~-ratio of atmosphere to ocean grids. We will refer to this configuration as GC2.1-
30 N512O12 (i.e., increased atmosphere and ocean resolution).

31

1 The differences between ORCA025 and ORCA12 in GC2.1 are:

- 2 • a reduction in the time step from 1200s to 240s
- 3 • a reduction in the isoneutral tracer diffusion from $300 \text{ m}^2\text{s}^{-1}$ to $125 \text{ m}^2\text{s}^{-1}$
- 4 • a reduction in the bilaplacian viscosity from $-1.5 \times 10^{11} \text{ m}^2\text{s}^{-1}$ to $-1.25 \times 10^{10} \text{ m}^2\text{s}^{-1}$

5 We note here that the parameter settings in GC2.1-N512O12 have not been tuned for the
6 coupled model; the model was run using the majority of parameter settings from the forced
7 ocean-only ORCA12 runs of Marzocchi et al. (2015). While reducing the isoneutral tracer
8 diffusivity is consistent with the increase in resolution, we note that results may have some
9 sensitivity to its magnitude. Experiments to investigate the impact of this parameter in GC2
10 were not performed but will be pursued in future work with GC3 (the next version of the
11 coupled model).

12 GC2.1-N512O12 was found to be very sensitive to features that had not proved to be a
13 problem in previous ocean-only integrations (e.g., Marzocchi et al., 2015). For example, the
14 model became unstable on the east coast of the UK every 6-12 months of simulation due to
15 extreme values in the velocity field, likely due to the lack of tidales dissipation in the model
16 which is are very important in this region. The model was restarted from these failures with a
17 small random perturbation to the atmosphere temperatureie-theta field in a similar way to
18 treatment of “grid-point instabilities” previously seen in atmosphere models (e.g., Mizielinski
19 et al 2014). The underlying problem with this unstable ocean point will be addressed in future
20 developments of the ORCA12 configuration.

21 The GC2 and GC2.1 experiments were run for 20 years with fixed atmospheric radiative
22 forcing representative of the present day (with greenhouse gas and aerosol values for the year
23 2000). All experiments were initialised in the following way:

- 24 • atmosphere: N216 and N512 both from September year 18 of the model state of a
25 previous N512 GA6 (Walters et al., in prep) forced atmosphere integration with
26 forcing representative of the year 2000, so that the land surface properties are at quasi-
27 equilibrium;
- 28 • ocean: temperature and salinity from the EN3 observational dataset (Ingleby and
29 Huddleston, 2007) 2004-8 September average with velocities initialised to zero;
- 30 • sea ice: 20 year September mean from a HadGEM1 (Johns et al., 2006) experiment
31 representative of a period centred on 1978.

- These latter two are the standard method for initialisation of “present day” coupled simulations at the Met Office.

The choice of the most appropriate ratio between ocean and atmosphere resolution remains an open research question worthy of further study. Short (two year) integrations using both higher and lower atmosphere resolutions coupled to ORCA12 were completed, although due to the short length of the integrations, they are not analysed here. In particular, a configuration using an N768 (17km) atmosphere led to a marked increase in the frequency of the type of model instabilities described earlier (from 1-2 per year to 5-6 per year).

3 Impact of model resolution on surface properties, heat transport and ocean circulation

The results shown in this section derive from 20 year simulations of the four experiments described in table 1, initialised and forced in an identical way.

a. Surface Properties

The pattern of large-scale biases in SST fields in Hadley Centre coupled climate models have remained largely unchanged since the models first ran without flux correction (e.g., Gordon et al., 2000); the large-scale biases exhibit warming in the Southern Ocean, cooling in the North Pacific and North Atlantic and warming in upwelling/stratocumulus regions off the western coasts of South America and Africa. Many of these biases are also very common in other models (e.g. Small et al., 2014). In contrast to the pattern, the magnitude of the SST biases has changed between model versions; in particular, comparing GC2 and HadGEM2-AO (Figure 1 of Williams et al., 2015), shows that the magnitude of the Northern hemisphere cooling was reduced in GC2 while the magnitude of the Southern Ocean warming was increased.

The time-series of the global mean Top of Atmosphere (TOA) radiation imbalance in the four models (Figure 1a) shows that the experiments with high (N512) atmosphere resolution have TOAs that are generally higher at the start of the experiments. However after 20 years all the experiments are starting to converge to a similar net TOA, as the shortwave and long-wave components adjust. Although the TOA-SST relationship is poorly defined (since the TOA imbalance is related to the rate of change of net ocean heat content; Palmer and McNeill,

1 2014), the integrated effect of the higher net TOA in the N512 experiments can be seen in the
2 timeseries of the global mean SST (Figure 1b) with GC2-N512 and GC2.1-N512O12 having
3 higher global mean SSTs.

4 In spite of the differences in global mean SST, major changes to the pattern and magnitude of
5 SST biases are only seen with both high atmosphere and ocean resolution (Figure 2). In
6 GC2.1-N512-ORCA12, the large-scale underlying SST biases are reduced relative to GC2
7 and GC2.1 (Figure 3): the warm bias in the Southern Ocean; cold bias in North Atlantic and
8 North Pacific and warm biases in stratocumulus regions. Similar reductions in SST biases
9 with high atmosphere and ocean resolution were also seen in Small et al. (2015). The increase
10 in ocean resolution is key to this improvement: when only atmosphere resolution is increased
11 (compare Figures 2a and b), there is only a small reduction in the warm bias associated with
12 stratocumulus regions (west of South America and Africa), while increased coupling
13 frequency (compare Figures 2a and c) shows only minor changes in SST biases.

14 In GC2 there is a cold bias in the North Atlantic subpolar gyre (SPG), Greenland-Iceland-
15 Norwegian (GIN) Seas and the Arctic. GC2.1-N512O12 shows a warming of several degrees
16 in the SPG and GIN seas relative to GC2 (see reduced cold bias in Figure 2d) and a very large
17 warming in the Central Arctic. The warming in the Central Arctic is associated with a
18 warming in the subpolar gyre, enhanced northward heat transport into the Arctic and melting
19 back of the sea ice edge in the Arctic (see below).

20 Resolution appears to have less of an impact on Sea Surface Salinity (SSS; Figure 4).
21 Nevertheless, there are reductions in high salinity biases in the Indian Ocean and the Pacific
22 (in particular, in the salinity maximum in the subtropical gyre of the South Pacific) as well as
23 reductions in the Arctic biases (although these are very sensitive to the distribution of sea ice).

24

25 *b. Sea ice*

26 The changes to the SST also affect sea ice distribution in both hemispheres. The seasonal
27 cycle of ice extent in the Arctic (Figure 5a) shows that the warm SSTs in GC2.1-N512O12 at
28 high Northern latitudes reduce the ice extent throughout the year. The March ice
29 concentrations in the Arctic (Figure 6) clearly demonstrate that the impact on the sea ice is
30 concentrated in the GIN seas with the sea ice edge in GC2.1-N512O12 much further north
31 than seen in GC2 with the edge being north of Spitzbergen and into the Barents Sea.

1 In comparison, the reduction in the warm bias in the Southern hemisphere leads to only
2 modest increases in the total sea ice extent (Figure 5b); the overall warming bias associated
3 with the lack of super-cooled liquid clouds (Bodas-Salcedo et al., 2014; Bodas-Salcedo et al.,
4 in press) still dominates the melting of sea ice. The small increase in sea ice extent is very
5 inhomogeneous; indeed, some regions in the Southern Ocean such as the Weddell Sea
6 actually show reductions in sea ice extent in GC2.1-N512-ORCA12 (Figure 6). The
7 reduction in the Weddell Sea is associated with [the formation of a-polynyas](#) in that region (see
8 below).

9

10 *c. Sub-surface ocean drifts*

11 Conservation of heat within the climate system implies that the net heat uptake by the ocean
12 should nearly balance the net radiative imbalance at the TOA. GC2.1-N512O12 has the
13 highest TOA imbalance of the four models (Table 2) and therefore will have the greatest net
14 heat uptake. Both models with increased atmosphere resolution (GC2-N512 and GC2.1-
15 N512O12) have a higher TOA imbalance than the models with lower atmosphere resolution
16 (GC2 and GC2.1).

17 The global temperature profiles (Figure 7a) show that GC2-N512 and GC2.1-N512O12 do
18 indeed have greater increases in temperature as a function of depth than either of the low
19 resolution models (GC2 and GC2.1), which is consistent with the higher TOA imbalance. The
20 main difference between GC2-N512 and GC2.1-N512O12 is that the increase in heat uptake
21 extends deeper in GC2.1-N512O12. This difference is also apparent in the global mean SST
22 anomaly (Table 2); the SST anomaly for years 11-20 in GC2.1-N512O12 is 0.44 K compared
23 with 0.60 K in GC2-N512, while the TOA imbalance is 2.02 W/m² and 1.79 W/m²
24 respectively. This shows that the ORCA12 version of the model is able to transport heat to
25 depth more effectively.

26 [An increase in heat uptake in GC2.1-N512O12 relative to GC2-N512 is unexpected when](#)
27 [considering the results of Griffies et al. \(2015\). Griffies et al. \(2015\) show that an increase in](#)
28 [eddy activity produces upward eddy transport with a net effect of reduced heat uptake. Our](#)
29 [results do not show a similar result suggesting that either the mean circulation is more](#)
30 [effectively transporting heat downwards \(which is consistent with an increased overturning](#)
31 [circulation\) or perhaps that there is an increase in spurious diapycnal mixing. Producing a](#)
32 [budget analysis in the future would help to address this issue.](#)

1 The distribution of the subsurface temperature changes varies depending on the latitudinal
2 range. South of 30°S (Figure 7b), near surface warming is reduced in GC2.1-N512O12
3 relative to the other models. In the Tropics (30°S-30°N; Figure 7c), GC2.1-N512O12 shows
4 increased warming shallower than 500m relative to the low resolution models but reduced
5 relative to GC2-N512. The Tropics also show increased warming at depth in GC2.1-
6 N512O12. The largest increase in near surface temperatures in GC2.1-N512O12 relative to
7 the other models occurs north of 30°N (Figure 7d) with the surface warming displacing a cold
8 bias to deeper in the water column. The warming is particularly concentrated north of 65°N
9 (Figure 7e) where it has previously been shown that Arctic sea ice melts back.

10 Drifts in sub-surface salinity show that GC2.1-N512O12 generally has larger salinity drifts
11 between 500 and 1000m (Figure 8a) which is largely associated with the region south of 30°S
12 (Figure 8b). In the northern hemisphere, drifts in salinity between 1000 and 2000m are also
13 more pronounced in GC2.1-N512O12 than the other models (Figure 8d). In contrast, large
14 fresh biases north of 65°N in most of the models is much reduced in GC2.1-N512O12 (Figure
15 8e). Understanding salinity drifts and their relationship to freshwater forcing is complex (eg,
16 Pardaens et al. 2003) and this aspect of the model performance will require further
17 investigation.

18

19

20

21 *d. Mixed layer depths*

22 In general over the open oceans, the mixed layer depths¹ (Figure 6) are very similar across the
23 different models and it is in the deep water formation regions where we see inter-hemispheric
24 changes. Winter mixed layers in the Northern hemispheres in GC2.1-N512O12 show a
25 reduction in the North Atlantic subpolar gyre. Most notably, in GC2.1-N512O12 deep mixed
26 layers are less extensive south of Greenland than in GC2 and are confined to the centre of the
27 Labrador Sea. Similar changes in Labrador Sea deep convection have been seen in sensitivity
28 experiments when overflow properties are improved (Graham et al., in prep.). The deeper

¹ Mixed layer depth is calculated as the depth at which density changes by 0.01 kg m^{-3} relative to the density at 10m

Formatted: Superscript

Formatted: English (United Kingdom)

1 mixed layers in the Arctic in GC2.1-N512O12 are consistent with warmer SSTs and reduced
2 sea ice extent in that region exposing open water.

3 The similarity of the mixed layer depths across the Southern Ocean demonstrate that it is not
4 changes to the mixed layer depths that lead to a reduction in the Southern Ocean warm bias.
5 As mentioned in the previous section, in the Weddell Sea, GC2.1-N512O12 has very deep
6 mixed layers (maximum of 800m in the decadal mean) linked to the formation of a polynyas.
7 Polynya formation varies both spatially and on an interannual basis over the last 9 years of the
8 simulation (Figure 9); the polynya first appears in year 12 and persists for 5 years before
9 disappearing, starting to re-emerge in year 18 and reaching a depth of 2070m in year 20.
10 ~~which~~ The appearance of the polynya in this decade explains the lack of increase of sea ice
11 extent in that region (as seen in Figure 6). Deeper winter mixed layers in GC2.1-N512O12 are
12 also evident through the mid-latitudes in the formation zones for Sub-Antarctic Mode Waters
13 and Antarctic Intermediate Waters. These could be due to the reduced warm bias (cooler
14 SSTs) in these regions (Figure 2).

15

16 *e. Ocean Circulation*

17 The improvements seen in the large-scale SST biases with high atmosphere and ocean
18 resolution (Figure 3) represent an overall improvement in the model simulation with warming
19 in the Northern hemisphere and cooling in the Southern hemisphere. This pattern is
20 reminiscent of inter-hemispheric modes that occur as a result of changes in the large-scale
21 thermohaline circulation (Vellinga and Wu, 2004). The meridional overturning at 24°N in our
22 simulations increases by O(1.5 Sv)-changes-only in GC2.1 and in the GC2.1-N512O12, with
23 an increase of by a further O(1.53 Sv) (Table 2). At 30°S, a change of O(3 Sv) is only seen in
24 GC2.1-N512O12. both in the North and South Atlantic, and is therefore The enhanced
25 meridional overturning is therefore attributed to the increased ocean resolution in combination
26 with the increased coupling frequency. The changes in the meridional overturning circulation
27 (Figure 910) are dominated by changes in the cell associated with North Atlantic Deep Water
28 (NADW) with changes extending into the Southern hemisphere. Examination of the
29 overturning in density space would further support this analysis but this was not possible with
30 the diagnostics available from this simulation and will be addressed in future simulations.

31 At the northern end of the NADW cell, we see increases in the volume flux of dense
32 overflows between the GIN Seas and the Atlantic (Table 2) that are consistent with the

1 NADW cell being strengthened both by the GIN sea sources and better representation of sills.
2 The volume flux of overflow waters across Denmark Straits generally reduces fairly rapidly
3 in ORCA025 runs (Figure 110a) but in GC2.1-N512O12 the overflow remains closer to the
4 observed value of 2.9 - 3.7 Sv (Dickson and Brown, 1994; Macrander et al., 2005; [Jochumsen](#)
5 [et al., 2012](#)). This appears to also contribute to a deeper (as well as stronger) NADW outflow
6 in ~~GC2-N512O12 this model (Figure 10)~~ and ~~is almost certainly we suggest that this is likely~~
7 ~~to be~~ associated with the increased resolution of the topography in the region of the
8 overflows.

9 The Antarctic Circumpolar Current (ACC) usually drifts in the ORCA025 GC models from
10 an initial value of approximately 150 Sv to below 100 Sv (Figure 110b). Increased ocean
11 resolution counteracts that, with the ACC stabilising close to 130 Sv in ~~GC2-N512O12 this 20~~
12 ~~year experiment~~. This value is close to the observations ~~which that~~ suggest an ACC transport
13 of 137 ± 8 Sv (Cunningham et al., 2003; [Meredith et al., 2011](#)). The increase in the transport
14 in the ACC can be explained by changes in the density field; the meridional density gradients
15 across the ACC (not shown) are increased in GC2.1-N512O12 (with steeper isopycnals) than
16 in GC2. ~~which~~ This result is consistent with increased southward flow, and stronger
17 upwelling, of NADW to the north of the ACC ([Allison et al., 2011](#)) and increased convection
18 to the south of the ACC in the Weddell Sea ([Hirabara et al., 2012](#)). The Southern Ocean
19 winds (not shown) respond differently across the four simulations (including a small increase
20 in GC2.1-N512O12 and a decrease in GC2.1). ~~Jones et al. (2011) have shown that the~~
21 ~~transient response of the ACC to changes in winds can be seen within 10 years, suggesting~~
22 ~~that it is not surprising that we are able to detect changes in the ACC in this set of~~
23 ~~experiments. and investigating these changes, how they relate to the model internal variability~~
24 ~~and their impact on the simulation will be a topic of future research.~~

Formatted: Not Highlight

25

26 *f. Heat transport*

27 As described in Gordon et al. (2000), drifts in volume averaged ocean temperature can be
28 related to discrepancies between the actual heat transports by the ocean and the heat transport
29 implied by the surface fluxes, i.e.

$$30 \quad \frac{\partial \rho c_p \langle \theta \rangle}{\partial t} + \oint \rho c_p (\bar{v}\bar{\theta} + \overline{v'\theta'}) dS + \oint \rho c_p A_{iso} \nabla_{\rho} \theta dS = \int F dA, \quad (1)$$

1 where $\langle \theta \rangle$ is the volume integrated temperature, $\bar{v}\bar{\theta}$ and $\overline{v'\theta'}$ are the time mean and time
2 varying components of the ocean meridional heat transports, ρc_p is density multiplied by
3 specific heat capacity, A_{iso} is the ~~isoneutral diffusivity~~isopycnal diffusion, $\nabla_{\rho}\theta$ is the
4 isoneutral gradients of temperature, ~~and~~ F is the surface heat flux, $dS (=dx*dz)$ is the cross
5 sectional area (x and z denote the zonal and vertical directions) and dA is the surface area of
6 the region. For our purposes here, we make the assumption that the isoneutral fluxes are
7 generally smaller than the other terms (~~isoneutral~~isopycnal diffusive fluxes are very small when
8 integrated over full depth).

9 Figure 12a shows the global northward heat transport in all four simulations. There are some
10 changes in the northern hemisphere in the GC2.1 simulation with the change to hourly
11 coupling, while changes in the southern hemisphere are only seen in GC2.1-N512O12
12 suggesting that these changes are driven by the increase in ocean resolution. The reduction in
13 southward heat transport in GC2.1-N512O12 centred at 45°S is highly unusual; although the
14 change does not lie outside interannual variability, a change of this magnitude in the multi-
15 year mean heat transport has not been seen in any other development runs of the GC series.
16 The modelled changes in the heat transports suggest that ocean processes are important in this
17 region, which is particularly relevant given the uncertainty in surface heat fluxes in the
18 Southern Ocean (Cerovecki et al., 2011). The ~~increase~~change in total heat transport comes
19 primarily from the time mean heat transport (not shown). This suggests that ~~increased changes~~
20 ~~in~~ resolution has ~~ve led to a change in~~ either ~~changed~~ the mean circulation or the temperature
21 profile. ~~In contrast, if the (as opposed to a increased heat transport was) change due to in~~
22 the time varying heat transport, ~~this which~~ would imply a direct role ~~for of the~~ mesoscale eddies).
23 As seen in previous sections, GC2.1-N512O12 shows changes in both the circulation and the
24 temperature profiles. The decreased southward heat transport in the Southern Ocean of
25 GC2.1-N512O12 could – at least partly - explain the reduced warm bias.

26 By comparing actual ocean heat transports with those implied by surface fluxes (i.e., the
27 second term of the left-hand side of Eqn. 1 with the right-hand side of Eqn. 1), this gives an
28 indication of the volume averaged drift in temperature (first term on the left-hand side of Eqn.
29 1). To remove the effect of the net radiative imbalance, the implied ocean heat transport is
30 calculated by subtracting the globally averaged imbalance from the surface fluxes before
31 integrating zonally and meridionally. This is equivalent to removing a globally integrated
32 temperature drift from the left-hand side of Eqn. 1. This can be described as:

$$\frac{\partial \rho c_p \langle \theta \rangle - \bar{\theta}}{\partial t} + \oint \rho c_p (\bar{v}\bar{\theta} + \overline{v'\theta'}) dS = \int (F - \bar{F}) dA, \quad (2)$$

where $\bar{\theta}$ and \bar{F} are the global mean temperature and surface flux respectively. Eqn. 2 shows that a residual imbalance between the implied and actual ocean heat transports is indicative of local temperature drifts. Both globally and in the Atlantic basin (Figure 12a,b) GC2.1-N512O12 can be seen to be as close to local balance as any of the other models, suggesting that the net drifts will be of a similar magnitude (in agreement with Figure 5).

Ocean resolution is the driving factor in a 0.2PW increase in the northward heat transport in the Atlantic; the modelled heat transports in GC2.1-N512O12 are generally within the error bars of the observations (Ganachaud and Wunsch, 2003; Figure 12b) in contrast to the other models with the lower resolution ocean component. The change in heat transport is linked to an increase in the overturning circulation (previous section), which is unsurprising given the dominant role of the meridional overturning circulation in the Atlantic heat transport (Hall and Bryden, 1982).

14

15 4 Summary and Discussion

16 In this paper we have shown results from a coupled climate model with an eddy resolving
 17 (1/12°) ocean component coupled to a high resolution (25 km) atmosphere component. When
 18 the SST bias from this climate simulation is compared to that from the Met Office standard
 19 resolution climate model, with eddy permitting (1/4°) ocean component and 60km atmosphere
 20 component, it is apparent that major SST biases in the Southern Ocean and North Atlantic and
 21 North Pacific have been reduced. Comparable experiments increasing only the atmosphere
 22 resolution or the coupling frequency, demonstrate that increased ocean resolution is the key
 23 driver for this change.

24 At the enhanced ocean resolution, the ocean circulation leads to increased poleward ocean
 25 heat transport in the Northern hemisphere and reduced poleward ocean heat transport in the
 26 Southern hemisphere. The change in the northward heat transport is driven at least in part by
 27 an enhanced NADW cell ~~which also contributes to maintaining the ACC front.~~ The stronger
 28 ACC front is maintained in spite of the expectation that improved representation of eddies in
 29 the Southern Ocean could lead to slumping of the front, this is at least in part associated with
 30 at high resolution may be associated with a number of factors: enhanced windstresses,
 31 increased at high resolution deep water formation in the Weddell Sea due to the presence of a

1 | polynya, enhanced southward transport of NADW and eddy fluxes. Changes in the global
2 | heat transports produce a shift in the large-scale biases, cooling the Southern Ocean and
3 | warming the North Atlantic and North Pacific. We have shown that heat penetrates deeper in
4 | our 1/12° model; Griffies et al. (2015) have demonstrated that mesoscale eddies transport heat
5 | upwards so it is likely that the increased transport of heat to depth is achieved by the time-
6 | mean as seen in transient experiments such as Banks and Gregory (2006). Future work will be
7 | focused on understanding the relative roles of resolving overflow topography (Behrens,
8 | 2013), eddy processes within the ocean including compensation and saturation (e.g., Munday
9 | et al., 2013) and air-sea interaction on the eddy scale (Roberts et al., in prep.) in driving the
10 | large-scale changes.

11 | Relative to the recent high resolution results of Small et al. (2014) and Griffies et al. (2015),
12 | our results emphasise the importance of increasing both ~~atmosphere and~~ ocean resolution and
13 | coupling frequency. Griffies et al. (2015) show smaller reductions in SST biases than seen
14 | here when moving from 1/4° to 1/10° resolution presumably related to keeping the
15 | atmosphere resolution unchanged. Enhanced coupling frequency along with enhanced vertical
16 | resolution near the air-sea interface both in the ocean (Megann et al., 2014) and atmosphere
17 | (Walters et al., in prep) is one feature of our model setup that is missing in Small et al. (2014).
18 | These aspects of the model setup may be especially important in regions of strong air-sea
19 | interaction including the stratocumulus regions where we see large improvements in the
20 | GC2.1-N512O12 simulation. ~~Overall, the improvements seen in this paper~~ Further work is
21 | required to quantify whether a combination of high resolution in ~~the both~~ atmosphere
22 | component is necessary in combination with ~~and the high resolution~~ ocean components ~~and~~
23 | well as high frequency coupling to produce the results described in this paper.

24 | As described in ~~the previous~~ section 2, one of the changes to the ocean model at higher
25 | resolution was a reduction in the isoneutral diffusivity~~on~~. Pradal and Gnanadesikan (2014)
26 | show that a reduction in the isoneutral diffusivity~~on~~ from 800 m²s⁻¹ to 400 m²s⁻¹ in a coarse
27 | resolution climate model is associated with cooling of order 1°C at high latitudes after 500
28 | years. ~~Given While that~~ the results here ~~may~~ exhibit some consistency with those of Pradal
29 | and Gnanadesikan (2014) in the Southern Ocean, further work is required to quantify the role
30 | of isoneutral diffusivity in producing the change in isopycnal diffusion is believed to be a
31 | secondary effect due to the fact that we are seeing a comparable or larger changes in SST on
32 | decadal timescales in a short 20-year run.

1 One caveat of these results is that the parallel simulations lasted only 20 years. However, ~~the~~
2 ~~close agreement between implied and actual meridional heat transports, suggests that the~~
3 ~~models are close to quasi-equilibrium. Additionally,~~ the broad similarity of the results
4 presented here compared with those of Small et al. (2014) from over 100 years of simulation
5 suggest that the results are reasonably robust. In terms of model drift, climate models
6 typically have a fast adjustment within the first five years (Sanchez-Gomez et al., 2016).
7 Large adjustments over the first 20 years are generally followed by a multi-centennial drift
8 towards equilibrium between ocean properties and the net TOA flux (Banks et al., 2007).
9 Longer simulations and further analyses will enable the robustness of the results presented
10 here (including wind-SST feedbacks) to be more fully understood.

11 In the results presented here, the 1/12° ocean model, which has a resolution of approximately
12 7 km at mid-latitudes, is coupled to an N512 atmosphere model, which has a resolution of 25
13 km. The relative importance of the atmosphere and ocean resolution remains a question which
14 will continue to be addressed in the community. We suggest that an~~An~~ atmosphere:ocean
15 ratio of 4:1 may be too high for the atmosphere to fully ~~respond to~~capture the details of the
16 ocean mesoscale. Future work will investigate the impact of coupling to even higher
17 resolution atmosphere models to investigate the role of the atmosphere:ocean ratio.

18 As we move towards ~~seamless coupled prediction,~~ using coupled models for prediction on
19 timescales from days to centuries, the results presented here are highly relevant to prediction
20 up to decadal timescales where data assimilation is employed. A coupled model that more
21 faithfully produces the current state of the ocean will rely less on data assimilation for
22 correcting large-scale biases and ~~be more able to include the representation of~~ better represent
23 spatial anomalies that control the large-scale variability. While there are many regions where
24 subsurface drifts are improved at ORCA12~~this~~ resolution, reducing the drifts seen in mid-
25 depth salinity will be important.

26 The ocean data assimilation scheme used in Met Office systems is called NEMOVAR,
27 employed in a 3DVar first-guess-at-appropriate-time (FGAT) mode (Waters et al., 2015). A
28 new version of NEMOVAR has recently been developed (Weaver et al. 2016) which uses a
29 2D implicit diffusion operator to model the horizontal background error covariances, one of
30 the most computationally expensive aspects of the scheme. This new version has been
31 developed in such a way that the number of costly global communications are minimised and
32 is therefore expected to scale well with resolution. Preliminary implementations of this

Formatted: Font color: Auto

1 scheme in the ORCA12 configuration indicate that it will be feasible to implement it for
2 operational ocean forecasting applications.

3 A key question for these timescales is whether employing enhanced resolution will address
4 the known problem of low signal-to-noise ratios (Eade et al., 2014) that has led to the need for
5 large ensembles for seasonal to decadal forecasting in lower resolution systems. Future work
6 to understand the drivers of large-scale bias reduction will support targeted experiments to
7 address the relative roles of resolution and ensemble size at these timescales. That said, ocean
8 resolution is clearly not going to solve all the issues in climate models; atmosphere errors
9 often dominate surface biases and, even at high resolution, ocean models need improved
10 representation of sub-gridscale processes.

13 **Code availability**

14 The MetUM is available for use under licence. A number of research organizations and
15 national meteorological services use the MetUM in collaboration with the Met Office to
16 undertake basic atmospheric process research, produce forecasts, develop the MetUM code
17 and build and evaluate Earth system models. For further information on how to apply for a
18 licence see <http://www.metoffice.gov.uk/research/collaboration/um-collaboration>. JULES is
19 available under licence free of charge. For further information on how to gain permission to
20 use JULES for research purposes see <https://jules.jchmr.org/software-and-documentation>. The
21 model code for NEMO v3.4 and v3.5 is available from the NEMO website ([www.nemo-](http://www.nemo-ocean.eu)
22 [ocean.eu](http://www.nemo-ocean.eu)). On registering, individuals can access the code using the open source subversion
23 software (<http://subversion.apache.org/>). The model code for CICE is freely available
24 (<http://oceans11.lanl.gov/trac/CICE/wiki/SourceCode>) from the United States Los Alamos
25 National Laboratory. In order to implement the scientific configuration of GC2/GC2.1 and to
26 allow the components to work together, a number of branches (code changes) are applied to
27 the above codes. Please contact the authors for more information on these branches and how
28 to obtain them.

30 **Appendix A: Model vertical levels**

31 The sensitivity to vertical resolution is not explored in this paper. However, a reduced
32 description of the vertical levels in GA6 (Table A1) and GO5 (Table A2) are included to

1 allow comparison with other models. For the full vertical levels, see Walters et al. (in prep.)
2 and Megann et al. (2014), respectively.

3

4

Level	Rho_height (m)
1	10.00
10	730.00
20	2796.67
30	6196.67
40	10930.12
50	17012.40
60	24710.70
70	35927.89
80	58978.35
85	82050.01

5 Table A1: Reduced list of level in GA6 which has 85 vertical levels

6

Formatted: Justified, Space Before: 6 pt, Line spacing: 1.5 lines

1

Level	Depth (m)	Thickness (m)
1	0.51	1.02
10	13.99	2.37
20	61.11	7.58
30	180.55	18.27
40	508.64	53.76
50	1387.38	125.29
60	2955.57	181.33
65	3897.98	194.29
70	4888.07	200.97
75	5902.06	204.23

2 Table A2: Reduced list of levels and layer thicknesses in GO5 which has 75 vertical levels

3

1 **Appendix B: Model performance and technical aspects**

2 The GC2.1 configuration was the first in which several further technical components of the
3 coupled system were considered essential to make the simulation manageable. The coupler
4 was upgraded from OASIS3 to OASIS3-MCT (Valcke et al, 2015) in order to improve
5 parallelisation of the coupling, particularly given the increased coupling frequency.

6 ORCA025 files are typically written as one file per processor by standard GC2 configurations
7 and combined into a single file prior to analysis as a post processing step. However, as HPC
8 parallel file systems are generally tuned for high bandwidth on large files and as GC2.1-
9 N512O12 configurations allocate 50 of the 80 nodes used by the full coupled system to the
10 ocean, this led to performance and functional issues when running on 1600 or more cores.
11 The NEMO XIOS diagnostic server (Madec, 2014) provides an asynchronous IO server
12 capability that allows the diagnostic files to be output as fewer larger files (although the
13 restart files are still written as one file per processor). Its introduction in the model allowed us
14 to overcome the limitations of the file system.

15 Land suppression was used for the NEMO and CICE models, so that processors are only
16 assigned to regions with active ocean points. This leads to a significant gain in core count,
17 although it meant that the automated large-scale diagnostics usually produced by NEMO
18 (zonal mean heat transports, meridional overturning) could not be generated.

19 Data volumes from this experiment were particularly large due to the output of additional
20 hourly and 3-hourly fluxes in order to examine the coupling processes in more detail. Each
21 month of model output comprised: ocean monthly mean files (netCDF) of 87GB together
22 with 6GB of daily files, sea-ice output (netCDF) of 57GB per month (with an additional
23 48GB of hourly output), and atmosphere output (PP format) of 100 GB per month. In total,
24 the 20 years of simulation produced 85 TB of data.

25 Little optimisation of the model was attempted since GC2.1 is not intended to be supported in
26 the long-term. Its successor, GC3, will be used for CMIP6. The GC2.1-N512O12 model used
27 80 full nodes (each of 32 cores) of an IBM Power 7 HPC, of which 55 were allocated to the
28 ocean/sea ice component (including 5 for the IO servers) and 25 for the atmosphere/land
29 component. The model throughput was 4 months per wall-clock day.

30 For previous model resolutions, the SCRIP utility (Jones, 1998) was used to generate the
31 conservative remapping files used to regrid coupling data between the ocean and atmosphere

1 grids (for temperature and fluxes), with bilinear interpolation used for the winds and surface
2 currents. However, due to the size of the high resolution grids used here, and the serial nature
3 of SCRIP, a different method was required. ESMF (ESMF, 2014; a package of parallelised
4 tools that use the same input grid descriptions as SCRIP, but can be run in parallel) was
5 therefore used to generate the remapping weights.

6

7

8 **Acknowledgements**

9 [We thank the Editor and the two reviewers \(Stephen Griffies and Andy Hogg\) for their](#)
10 [constructive comments. Matt Martin provided useful input on data assimilation for ORCA12.](#)

11 This work was primarily supported by the Joint DECC/Defra Met Office Hadley Centre
12 Climate Programme (GA01101). Part of the work was undertaken with National Capability
13 funding from NERC for ocean modelling. We acknowledge use of the MONSooN system, a
14 collaborative facility supplied under the Met Office-NERC Joint Weather and Climate
15 Research Programme (JWCRP). Met Office authors were supported by the joint UK
16 DECC/DEFRA Met Office Hadley Centre Climate Programme (GA01101). MR
17 acknowledges support from the EU FP7 IS-ENES2 project for work on ESMF and regriding
18 tools. We acknowledge the considerable effort on development and evaluation of ORCA12 by
19 the DRAKKAR community. HH thanks IH.

20

21

22 **References**

23 [Allison, L. C., Johnson, H. L. and Marshall, D. P.: Spin-up and adjustment of the Antarctic](#)
24 [Circumpolar Current and global pycnocline, J. Mar. Res., 69, 167-189, 2011.](#)

25 Banks, H. T. and Gregory, J. M.: Mechanisms of ocean heat uptake in a coupled climate
26 model and the implications for tracer based predictions of ocean heat uptake, Geophys. Res.
27 Lett., 33, L076208, doi:10.1029/2005GL025352, 2006.

28 Banks, H. T., Stark, S. and Keen, A. B.: The adjustment of the coupled climate model
29 HadGEM1 towards equilibrium and the impact on global climate, J. Climate, 20, 5815-5826,
30 2007.

1 Behrens, E.: The oceanic response to Greenland melting: the effect of increasing model
2 resolution, PhD thesis, University of Kiel, 2013.

3 Best, M. J., Pryor, M., Clark, D. B., Rooney, G. G., Essery, R. L. H., Ménard, C. B., Edwards,
4 J. M., Hendry, M. A., Porson, A., Gedney, N., Mercado, L. M., Sitch, S., Blyth, E., Boucher,
5 O., Cox, P. M., Grimmond, C. S. B., and Harding, R. J.: The Joint UK Land Environment
6 Simulator (JULES), model description – Part 1: Energy and water fluxes, *Geosci. Model*
7 *Dev.*, 4, 677–699, doi:10.5194/gmd-4-677-2011, 2011

8 Bodas-Salcedo, A., Williams, K. D., Ringer, M. A., Beau, I., Cole, J. N. S., Dufresne, J.-L.,
9 Koshiro, T., Stevens, B., Wang, Z. and Yokohata, T.: Origins of the solar radiation biases
10 over the Southern Ocean in CFMIP2 models, *J. Climate*, 27, 41-56, doi:10.1175/JCLI-D-13-
11 00169.1., 2014.

12 Bodas-Salcedo, A., Hill, P. G., Furtado, K., Karmalkar, A., Williams, K. D., Field, P. R.,
13 Manners, J. C., Hyder, P. and Kato, S.: Large contribution of supercooled liquid clouds to the
14 solar radiation budget of the Southern Ocean, *J. Climate*, in press.

15 Bryan, F. O., Tomas, R., Dennis, J. M., Chelton, D. B., Loeb N. G. and McClean J. L.:
16 Frontal scale air-sea interaction in high-resolution coupled climate models, *J. Clim.*,
17 doi:10.1175/2010JCLI3665.1, 2010.

18 Cerovecki, I., Talley, L. D., Mazloff, M. R.: A Comparison of Southern Ocean Air-Sea
19 Buoyancy Flux from an Ocean State Estimate with Five Other Products. *Journal of Climate*.
20 24:6283-6306, 2011.

21 Chelton, D. B. and Xie, S.-P.: Coupled ocean-atmosphere interaction at oceanic mesoscales,
22 *Oceanography*, 23(4), 52-69, 2010.

23 Chelton, D. B., Schlax, M. G. and Samelson, R. M.: Global observations of nonlinear
24 mesoscale eddies, *Prog. Oceanogr.*, 91, 167-216, 2011.

25 Cunningham, S. A., Alderson, S. G., King, B. A. and Brandon, M. A.: Transport and
26 variability of the Antarctic Circumpolar Current in Drake Passage, *J. Geophys. Res.*, 108,
27 doi:10.1029/2001JC001147, 2003.

28 Delworth, T. L., Rosati, A., Anderson, W. G., Adcroft, A., Balaji, V., Benson, R., Dixon, K.
29 W., Griffies, S. M., Lee, H.-C., Pacanowski, R. C., Vecchi, G. A., Wittenberg, A. T., Zeng,

1 F., and Zhang, R.: Simulated climate and climate change in the GFDL CM2.5 high-resolution
2 coupled climate model. *Journal of Climate*, 25(8), doi:10.1175/JCLI-D-11-00316.1, 2012.

3 Deshayes, J.,Treguier, A. -M., Barnier, B., Lecointre, A., Le Sommer, J, Molines, J.-M.,
4 Penduff, T., Bourdalle-Badie, R., Drillet, Y., Garric, G., Benshila, R., Madec, G., Biastoch,
5 A., Boening, C. W., Scheinert, M., Coward, A. C. and Hirschi, J. J.: Oceanic hindcast
6 simulations at high resolution suggest that the Atlantic MOC is bistable, *Geophys. Res. Lett.*,
7 40, 3069-3073 doi:10.1002/grl.50534, 2013.

8 Dickson R.R., Brown J.: The production of North Atlantic Deep Water: Sources, rates, and
9 pathways. *J Geophys Res* 99(C6):12,319–12,341, DOI 10.1029/94jc00530, 1994.

10 Eade, R., Smith D., Scaife A., Wallace E., Dunstone N., Hermanson L. and Robinson N.: Do
11 seasonal to decadal predictions underestimate the predictability of the real world?, *GRL*, DOI:
12 10.1002/2014GL061146, 2014.

13 ESMF: Earth System Modelling Framework Reference Manual for Fortran, 2014. Available
14 from
15 http://www.earthsystemmodeling.org/esmf_releases/public/ESMF_6_3_0rp1/ESMF_refdoc

16 Frenger, I., Gruber, N., Knutti, R. and Munnich, M.: Imprint of Southern Ocean eddies on
17 winds, clouds and rainfall, *Nature Geoscience*, 6, 608-612, 2013.

18 Ganachaud, A. and Wunsch, C.: Large-scale ocean heat and freshwater transports during
19 World Ocean Circulation Experiment, *J. Climate*, 16, 696-705, 2003.

20 Gordon C., Cooper, C., Senior, C. A., Banks, H., Gregory, J. M., Johns, T. C., Mitchell, J.
21 F. B., and Wood, R. A.: The simulation of SST, sea ice extents and ocean heat transports in a
22 version of the Hadley Centre coupled model without flux adjustments, *Climate Dynamics*, 16,
23 147-168, 2000.

24 Griffies, S. M., Winton, M., Anderson, W. G., Benson, R., Delworth, T. L., Dufour, C. O.,
25 Dunne, J. P., Goddard, P., Morrison, A. K., Rosati, A., Wittenberg, A. T., Yin, J. J. and
26 Zhang, R.: Impacts on Ocean Heat from Transient Mesoscale Eddies in a Hierarchy of
27 Climate Models, *J. Climate*, 28, 952-977, 2015.

28 Hall, M. M., and Bryden, H. L.: Direct estimates and mechanisms of ocean heat transport,”
29 *Deep-Sea Res.*, **29**, No. 3A, 339–359, 1982.

1 Hallberg, R.: Using a Resolution Function to Regulate Parameterizations of Oceanic
2 Mesoscale Eddy Effects. *Ocean Modelling*, 72, DOI:10.1016/j.ocemod.2013.08.007, 2013.

3 [Hallberg, R.: Numerical insabilities of the ice/ocean coupled system. *CLIVAR Exchanges*,](#)
4 [65, 38-42, 2014.](#)

5 Hewitt, H. T., Copsey, D., Culverwell, I. D., Harris, C. M., Hill, R. S. R., Keen, A. B.,
6 McLaren, A. J. and Hunke, E. C.: Design and implementation of the infrastructure of
7 HadGEM3: the next-generation Met Office climate modelling system, *Geosci. Model Dev.*, 4,
8 223-253, doi:10.5194/gmd-4-223-2011, 2011.

9 [Hirabara, M., Tsujino, H., Nakano, H. And Yamanaka, G.: Formation mechanisms of the](#)
10 [Weddell Sea Polynya and the impact on the global abyssal ocean, *J. Oceanography*, 68 \(5\),](#)
11 [doi:10.1007/s10872-012-0139-3, 2012.](#)

12 Hunke, E. C. and Lipscomb, W. H.: CICE: the Los Alamos sea ice model documentation and
13 software users' manual, Version 4.1, LA-CC-06-012, Los Alamos National Laboratory, N.M.,
14 2010.

15 Hunke, E. C., Lipscomb, W. H., Turner, A. K., Jeffery, N. and Elliott, S.: CICE: The Los
16 Alamos Sea Ice Model, Documentation and Software User's Manual, Version 5.1. Tech. Rep.
17 LA-CC-06-012, Los Alamos National Laboratory, Los Alamos, New Mexico. Available
18 from: <http://oceans11.lanl.gov/trac/CICE>, 2015.

19 Hurlburt, H. E., Brassington, G. B., Drillet, Y., Kamachi, M., Benkiran, M., Bourdalle-Badie,
20 R., Chassignet, E. P., Jacobs, G. A., Le Galloudec, O., Lellouche, J. M., Metzger, E. J.,
21 Smedstad, O. M., and Wallcraft, A. J.: High-Resolution Global and Basin-Scale Ocean
22 Analyses and Forecasts, *Oceanography*, 22(3), 110-127, 2009.

23 Ingleby, B. and Huddleston, M.: Quality control of ocean temperature and salinity profiles -
24 Historical and real-time data. *J. Mar. Sys.*, 65, 158-175, 2007.

25 [Jones, D. C., Ito, T. and Lovenduski, N. S.: The transient response of the Southern Ocean](#)
26 [pycnocline to changing winds, *Geophys. Res. Lett.*, 38, L15604, doi:10.1029/2011GL048145,](#)
27 [2011.](#)

28 Jones P. W.: A User's Guide for SCRIP: A Spherical Remapping and Interpolation Package,
29 Version 1.5, Los Alamos National Laboratory, 1998.

1 [Jochumsen, K., Quadfasel, D., Valdimarsson, H. and Jonsson, S.: Variability of the Denmark](#)
2 [Strait overflow: Moored timeseries from 1996-2011, J. Geophys. Res., 117, C12003,](#)
3 [doi:10.1029/2012JC008244, 2012.](#)

4 Johns, T. C., Durman, C. F., Banks, H. T., Roberts, M. J., McLaren, A. J., Ridley, J. K.,
5 Senior, C. A., Williams, K. D., Jones, A., Rickard, G. J., Cusack, S., Ingram, W. J., Crucifix,
6 M., Sexton, D. M. H., Joshi, M. M., Dong, B. W., Spencer, H., Hill, R. S. R., Gregory, J. M.,
7 Keen, A. B., Pardaens, A. K., Lowe, J. A., Boda-Salcedo, A., Stark, S. and Searl, Y.: The new
8 Hadley Centre climate model HadGEM1: Evaluation of coupled simulations in comparison to
9 previous models, J. Climate, 19 (7), 1327–1353, 2006.

10 McClean, J. L., Bader, D. C., Bryan, F. O., Maltrud, M. E., Dennis, J. M., Mirin, A. A., Jones,
11 P. W., Kim, Y. Y., Ivanova, D. P., Vertenstein, M., Boyle, J. S., Jacob, R. L., Norton, N.,
12 Craig, A. and Worley, P. H.: A prototype two-decade fully-coupled fine-resolution CCSM
13 simulation. Ocean Modelling, 39:10-30. 10.1016/j.ocemod.2011.02.011, 2011.

14 Macrander, A., Send, U., Valdimarsson, H., Jonsson, S. and Kase, R. H.: Interannual changes
15 in the overflow from the Nordic Seas into the Atlantic Ocean through Denmark Strait.
16 Geophys Res Lett 32(6):L06,606+, DOI 10.1029/2004gl021463, 2005.

17 Madec, G.: "NEMO ocean engine". Note du Pôle de modélisation, Institut Pierre-Simon
18 Laplace (IPSL), France, No 27 ISSN No 1288-1619, 2014.

19 Marzocchi, A., Hirschi, J. J. M., Holliday, N. P., Cunningham, S. A., Blaker, A. T. and
20 Coward, A. C.: The North Atlantic subpolar circulation in an eddy-resolving global ocean
21 model. Journal of Marine Systems, 142, 126-143. 10.1016/j.jmarsys.2014.10.007, 2015.

22 Megann, A.P., Storkey, D., Aksenov, Y., Alderson, S., Calvert, D., Graham, T., Hyder, P.,
23 Siddorn, J. and Sinha, B.: GO 5.0: The joint NERC-Met Office NEMO global ocean model
24 for use in coupled and forced applications. Geosci. Model Dev., 7 (3). 1069-1092.
25 10.5194/gmd-7-1069-2014, 2014.

26 [Meredith, M.P., Woodworth, P. L., Chereskin, T. K., Marshall, D. P., Allison, L. C., Bigg, G.](#)
27 [R., Donohue, K., Heywood, K. J., Hughes, C. W., Hibbert, A., Hogg, A. McC., Johnson, H.](#)
28 [L., Jullion, L., King, B. A., Leach, H., Lenn, Y.-D., Morales Maqueda, M. A., Munday, D. R.,](#)
29 [Naveira Garabato, A. C., Provost, C., Sallee J.-B., and Sprintall, J.: Sustained monitoring of](#)
30 [the Southern Ocean at Drake Passage: past achievements and future priorities, Reviews of](#)
31 [Geophysics, 49, RG4005, doi:10.1029/2010RG000348, 2011.](#)

Formatted: No underline, Font color:
Text 1

Formatted: No underline, Font color:
Text 1

- 1 Minobe, S., Kuwano-Yoshida, A., Komori, N., Xie, S.-P. and Small, R. J.: Influence of the
2 Gulf Stream on the troposphere, *Nature*, 452, doi:10.1038/nature06690, 2008.
- 3 Mizielinski, M. S., Roberts, M. J., Vidale, P. L., Schiemann, R., Demory, M.-E., Strachan, J.,
4 Edwards, T., Stephens, A., Lawrence, B. N., Pritchard, M., Chiu, P., Iwi, A., Churchill, J., del
5 Cano Novales, C., Kettleborough, J., Roseblade, W., Selwood, P., Foster, M., Glover, M., and
6 Malcolm, A.: High-resolution global climate modelling: the UPSCALE project, a large-
7 simulation campaign, *Geosci. Model Dev.*, 7, 1629-1640, doi:10.5194/gmd-7-1629-2014,
8 2014.
- 9 Munday, D. R., Johnson, H. L. and Marshall, D. P.: Eddy saturation of equilibrated
10 circumpolar currents, *J. Phys. Oceanogr.*, 43, 507-532, 2013.
- 11 Palmer, M. D., and McNeall, D. J.: Internal variability of Earth's energy budget as simulated
12 by CMIP5 climate models, *Env. Res. Lett.*, 9 (3), 2014.
- 13 Pardaens A. K., Banks, H. T., Gregory, J. M. and Rowntree, P. R.: Freshwater transports in
14 HadCM3, *Climate Dynamics*, 21, 177-195, 2003.
- 15 Pradal, M.-A., and Gnanadesikan, A.: How Does the Redi Parameter for Mesoscale Mixing
16 Impact Global Climate in an Earth System Model? *Journal of Advances in Modeling the*
17 *Earth System*, 6:586-601, 2014.
- 18 Rae, J. G. L., Hewitt, H. T., Keen, A. B., Ridley, J. K., West, A. E., Harris, C. M., Hunke, E.
19 C. and Walters, D. N.: Development of Global Sea Ice 6.0 CICE configuration for the Met
20 Office Global Coupled Model, *Geosci. Model Dev.*, 8, 2221-2230, doi:10.5194/gmd-8-2221-
21 2015, 2015.
- 22 Sanchez-Gomez, E., Cassou, C., Ruprich-Robert, Y., Fernandez, E., and Teray, L.: Drift
23 dynamics in a coupled model initialized for decadal forecasts, doi :10.1007/s00382-015-2678-
24 y, *Clim. Dyn.*, 46, 1819–1840, 2016.
- 25 Sheldon, L., and Czaja, A.: Seasonal and interannual variability of an index of deep
26 atmospheric convection over western boundary currents. *Q J R Meteorol Soc* 140: 22–30. doi:
27 10.1002/qj.2103, 2014.
- 28 Small, R. J., Bacmeister, J., Bailey, D. A., Baker, A., Bishop, S., Bryan, F. O., Caron, J.,

1 Dennis, J., Gent, P. R., Hsu, H.-M., Jochum, M., Lawrence, D. M., Munoz Acevedo, E.,
2 diNezio, P., Scheitlin, T., Tomas, R., Tribbia, J., Tseng, Y. and Vertenstein, M.: A new
3 synoptic-scale resolving global climate simulation using the Community Earth System Model.
4 Journal of Advances in Modeling Earth Systems, 6, 1065-1094, DOI:
5 10.1002/2014MS000363, 2014.

6 Tréguier, A.-M., Deshayes, J., Lique, C., Dussin, R. and Molines, J.-M.: Eddy contributions
7 to the meridional transport of salt in the North Atlantic. Journal of Geophysical Research.
8 Oceans, Wiley-Blackwell, 117, doi:10.1029/2012JC007927, 2012.

9 Valcke, S., Craig, T. and Coquart, L.: OASIS3-MCT User Guide, OASIS3-MCT 3.0,
10 Technical Report, TR/CMGC/15/38, CERFACS/CNRS SUC URA No 1875, Toulouse,
11 France, 2015.

12 Vellinga, M. and Wu, P.: Low-Latitude Freshwater Influence on Centennial Variability of the
13 Atlantic Thermohaline Circulation. J. Climate, 17, 4498–4511, doi: 10.1175/3219.1, 2004.

14 Waters, J., Lea, D. J., Martin, M. J., Mirouze, I., Weaver, A. and While, J.: Implementing a
15 variational data assimilation system in an operational 1/4 degree global ocean model. Q.J.R.
16 Meteorol. Soc., 141: 333-349. doi: 10.1002/qj.2388, 2015,

Formatted: No underline, Font color:
Text 1

17 Weaver, A. T., Tshimanga, J. and Piacentini, A. : Correlation operators based on an implicitly
18 formulated diffusion equation solved with the Chebyshev iteration. Q.J.R. Meteorol. Soc.,
19 142: 455–471. doi: 10.1002/qj.2664, 2016,

Formatted: No underline, Font color:
Text 1

20 Williams, K. D., Harris, C. M., Bodas-Salcedo, A., Camp, J., Comer, R. E., Copsey, D.,
21 Fereday, D., Graham, T., Hill, R., Hinton, T., Hyder, P., Ineson, S., Masato, G., Milton, S. F.,
22 Roberts, M. J., Rowell, D. P., Sanchez, C., Shelly, A., Sinha, B., Walters, D. N., West, A.,
23 Woollings, T. and Xavier, P. K.: The Met Office Global Coupled model 2.0 (GC2)
24 configuration. Geosci. Model Dev., 8, 1509-1524, doi:10.5194/gmd-8-1509-2015, 2015.

Formatted: Font color: Text 1

25 Zhang Y. and Vallis, G. K.: Ocean Heat Uptake in Eddying and Non-Eddying Ocean
26 Circulation Models in a Warming Climate, J. Phys. Oceanogr., 43 (10), 2211-2229,
27 doi:10.1175/JPO-D-12-078.1, 2013.

28

1 Table 1. Coupled models used in this paper

Model	Horizontal Resolution	Coupling frequency
GC2 (Williams et al., 2015)	N216-ORCA025	3-hourly
GC2-N512	N512-ORCA025	3-hourly
GC2.1 (this paper)	N216-ORCA025	1-hourly
GC2.1-N512O12	N512-ORCA12	1-hourly

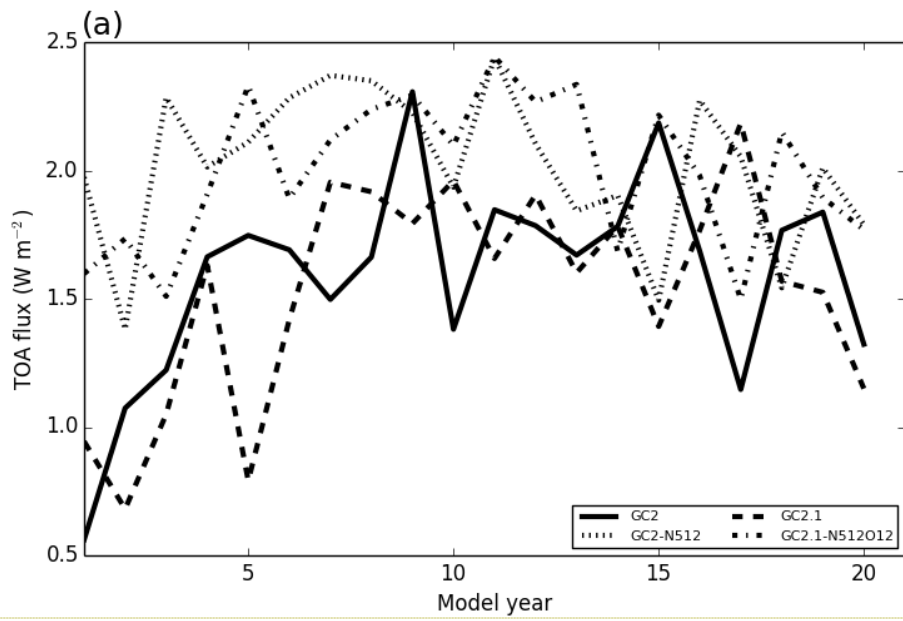
2

3

4 Table 2. Key metrics from years 11-20 of the experiments and observations. TOA
 5 observations from CERES/EBAF for years 2000-2010. Global mean SST error (compared to
 6 Reynolds OI). Overflows are calculated as southward flow across the Greenland-Iceland-
 7 Scotland ridge below density of 27.8 kg m^{-3} and have standard deviation shown in brackets.

Model	Net TOA (W/m^2)	Global mean SST error (K)	Maximum overturning at 30°S (Sv)	Maximum overturning at 24°N (Sv)	Net transport from overflows (Sv)
Observations	0.85				
GC2	1.61	0.25	13.7	14.6	4.0 (0.24)
GC2-N512	1.79	0.60	14.3	14.9	3.9 (0.28)
GC2.1	1.64	0.29	14.3	16.4	4.7 (0.26)
GC2.1- N512O12	2.02	0.44	17.5	17.7	5.9 (0.42)

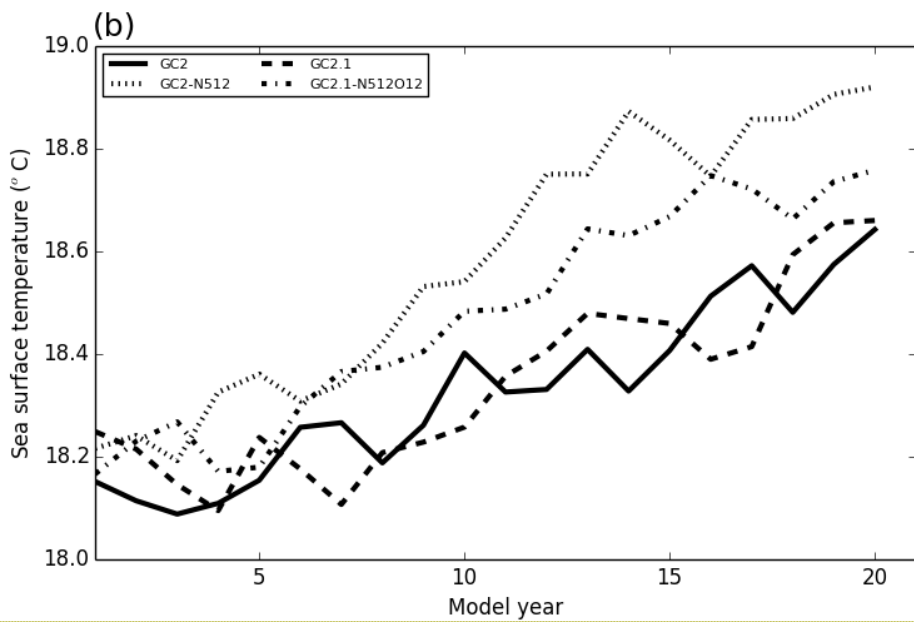
8



Formatted: No underline, Font color: Black

1

2

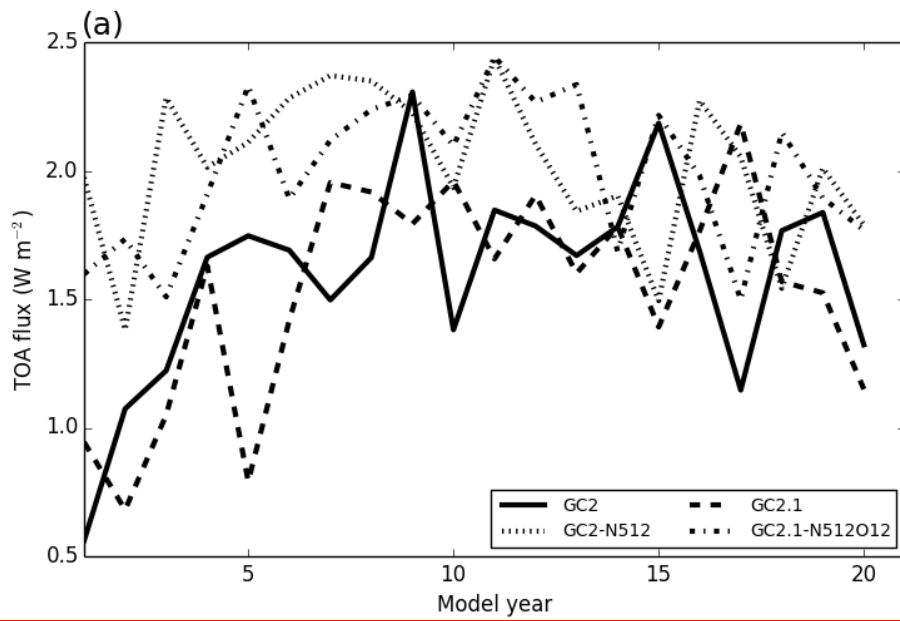


Formatted: No underline, Font color: Black

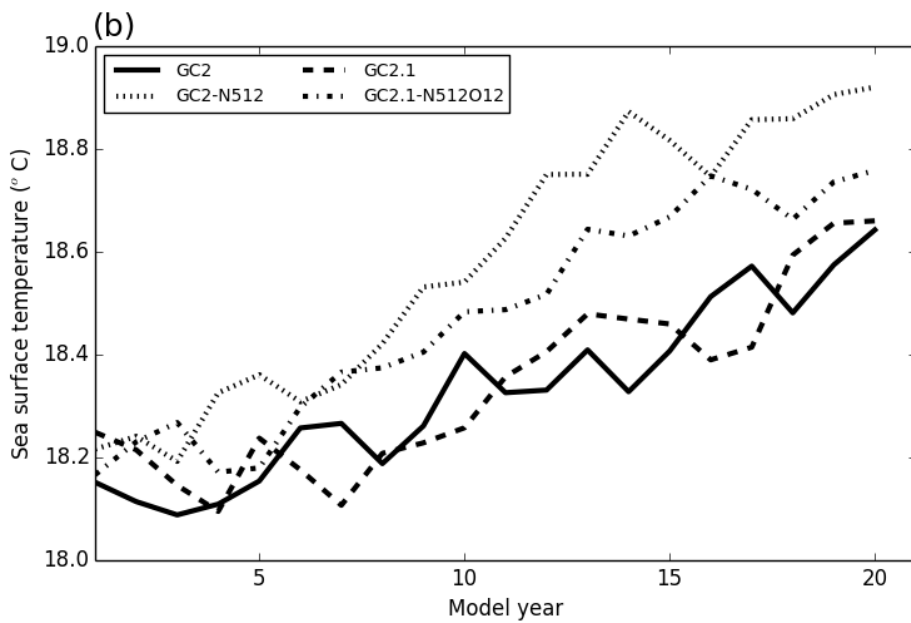
3

4

5

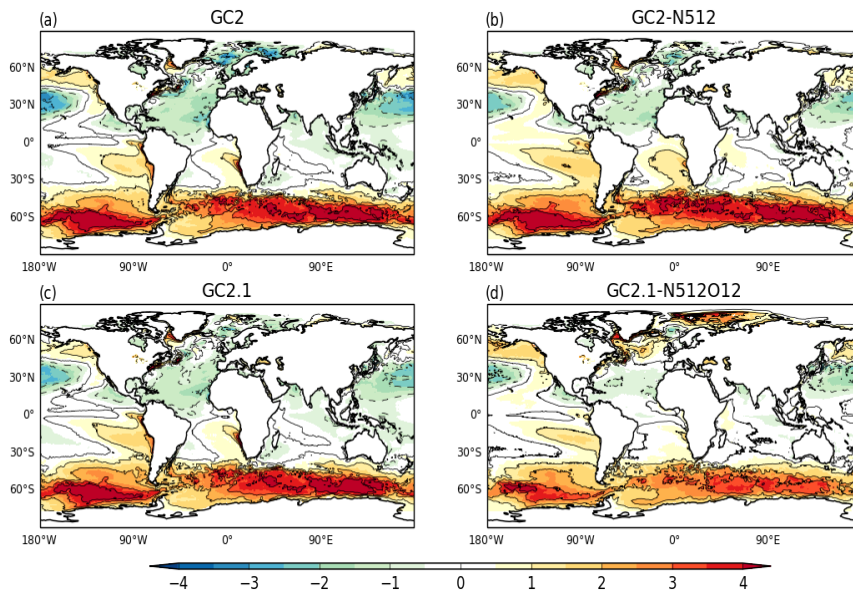


Formatted: No underline, Font color: Black

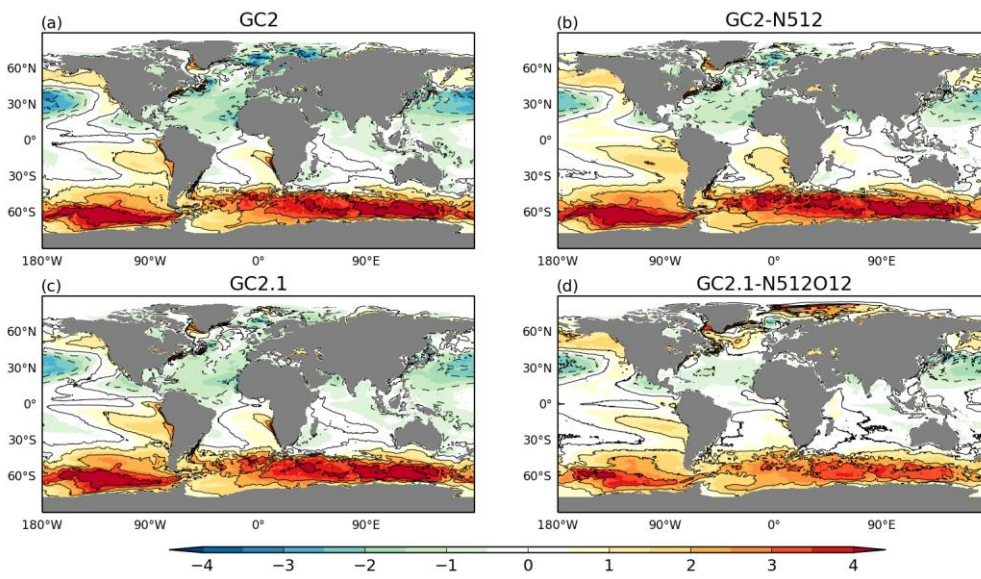


Formatted: No underline, Font color: Black

Figure 1: Timeseries of a) net TOA and b) global mean SST from GC2, GC2-N512, GC2.1 and GC2.1-N512O12.



Formatted: No underline, Font color: Auto



Formatted: No underline, Font color: Black

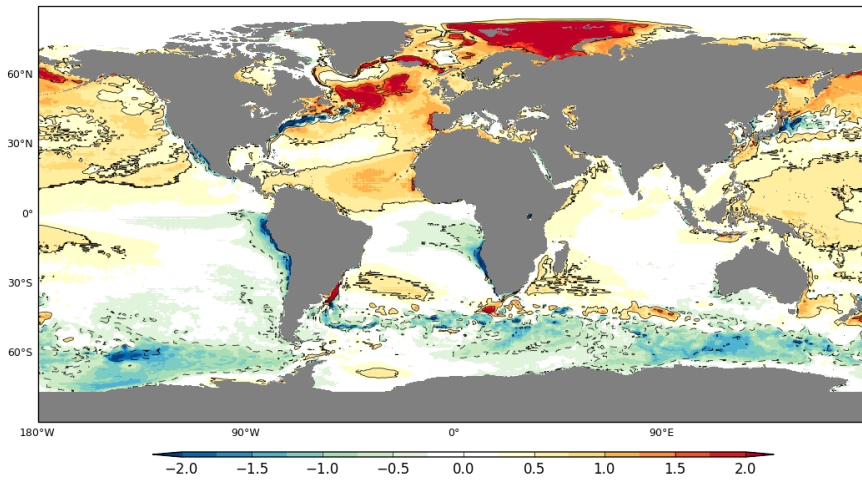
1

2

3 Figure 2: Differences between modelled SST from years 11-20 and observed SST from
 4 HadISST (°C) for a) GC2, b) GC2-N512, c) GC2.1 and d) GC2.1-N512O12.

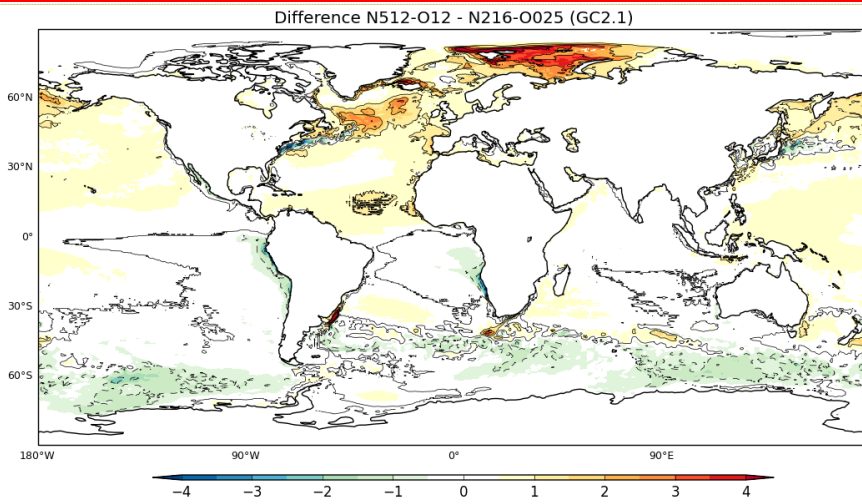
5

6



Formatted: No underline, Font color: Black

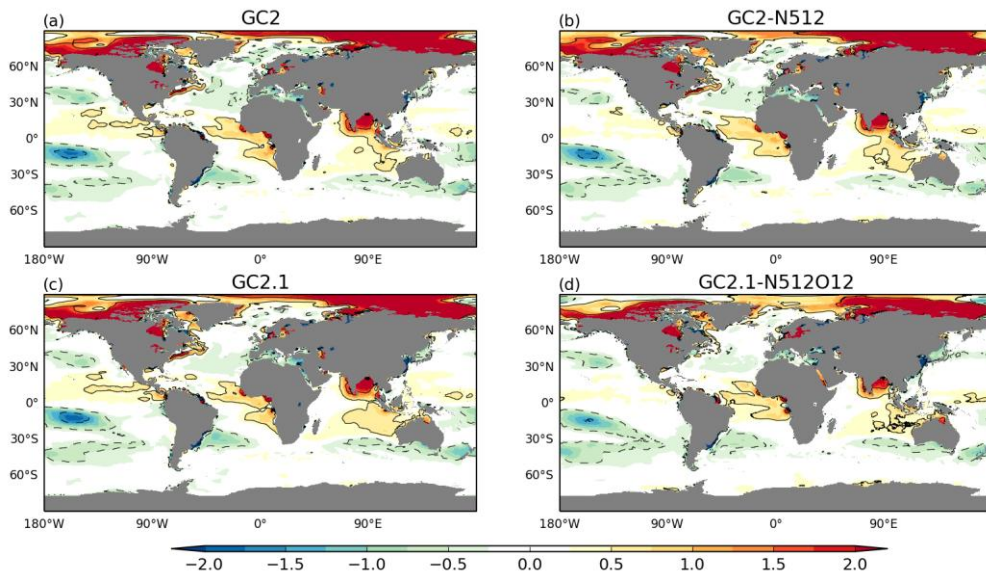
1



2
3

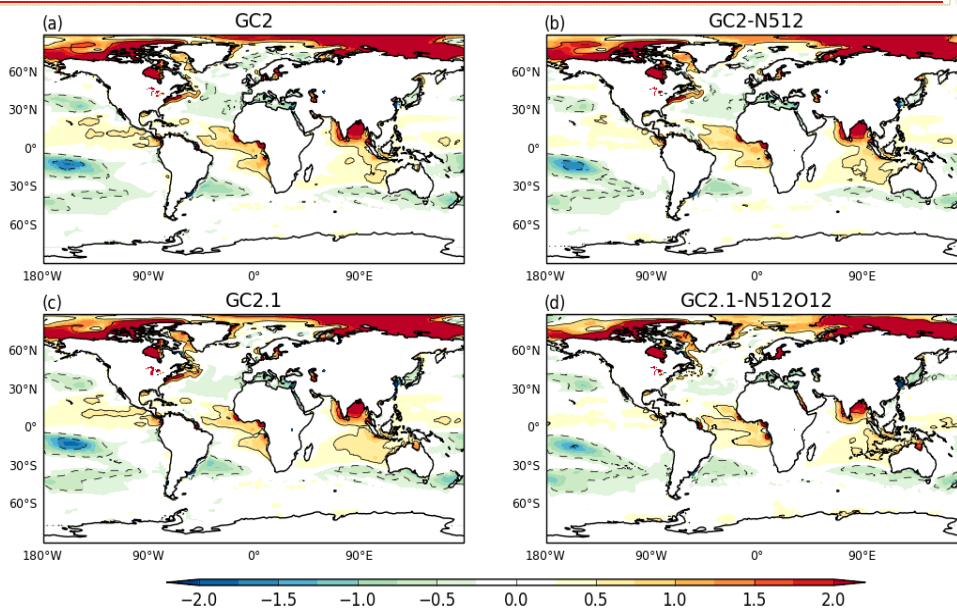
4 Figure 3: SST difference (°C) for years 11-20 between GC2.1-N512O12 and GC2.1

1



Formatted: No underline, Font color: Black

2

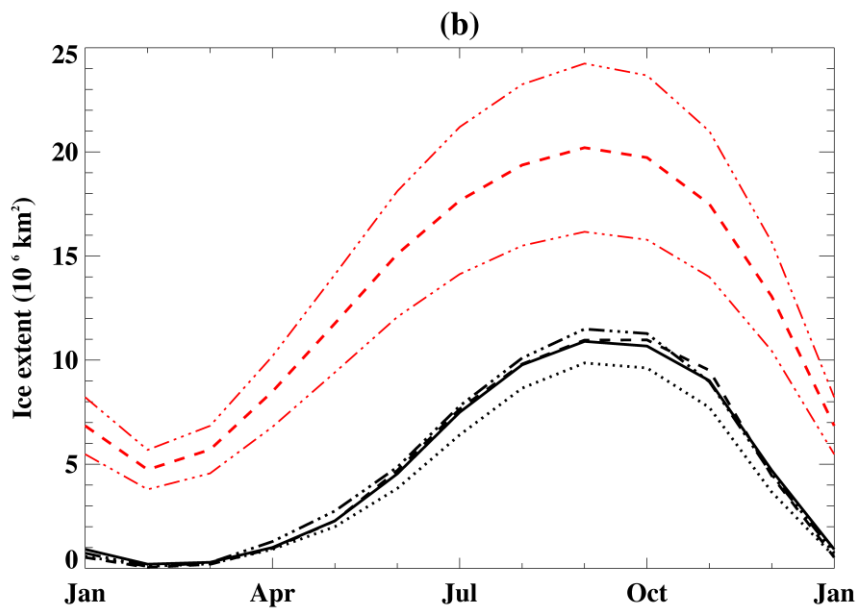
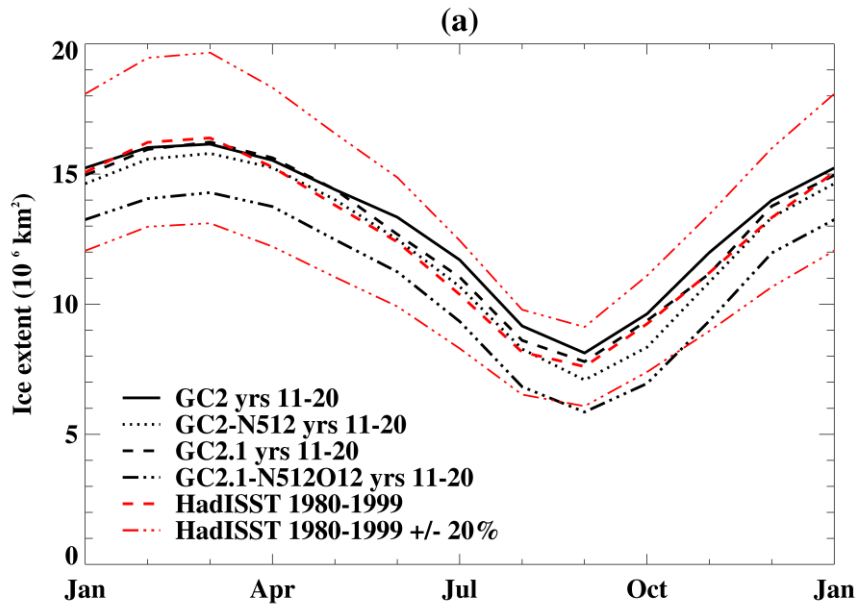


3

4

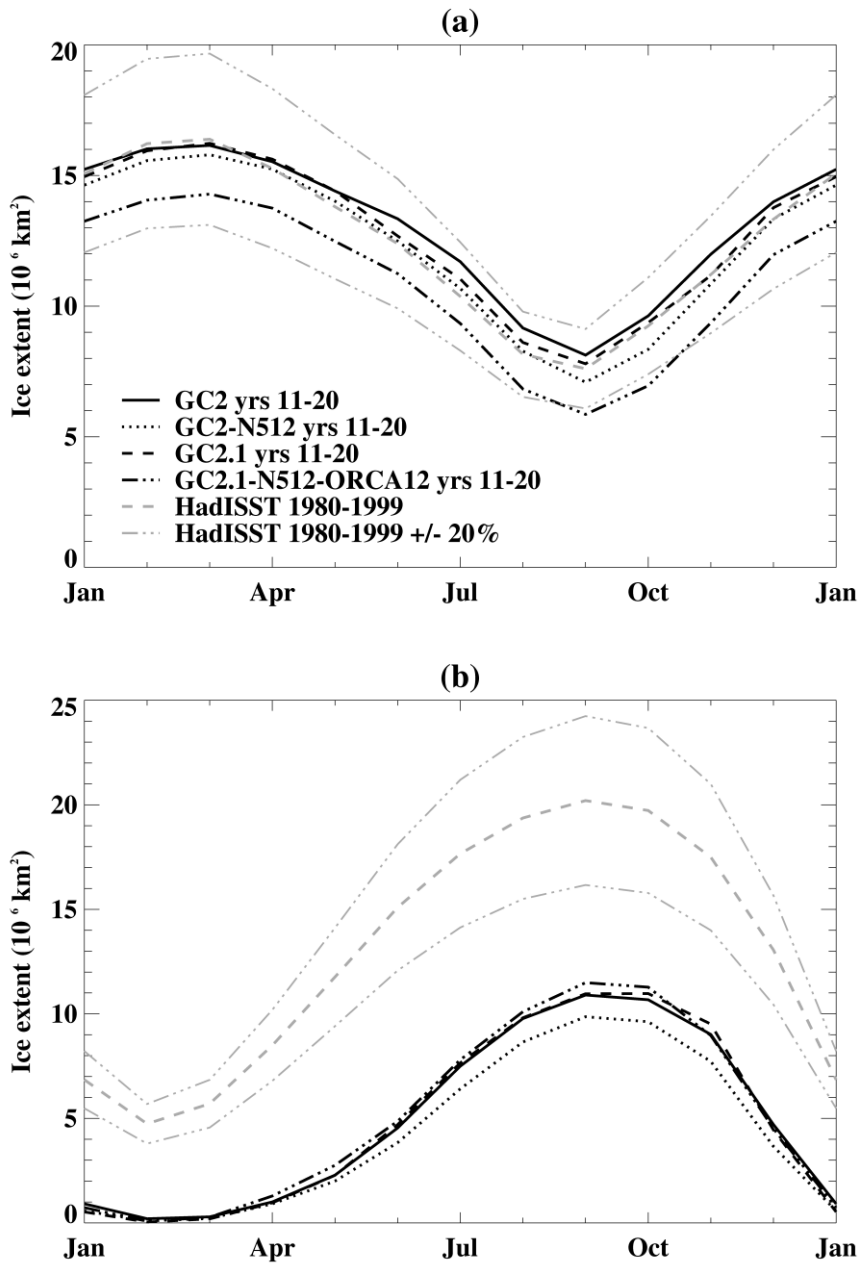
5 Figure 4: Differences between modelled SSS from years 11-20 and observed SSS from EN4
6 (psu) for a) GC2, b) GC2-N512, c) GC2.1 and d) GC2.1-N512O12.

7

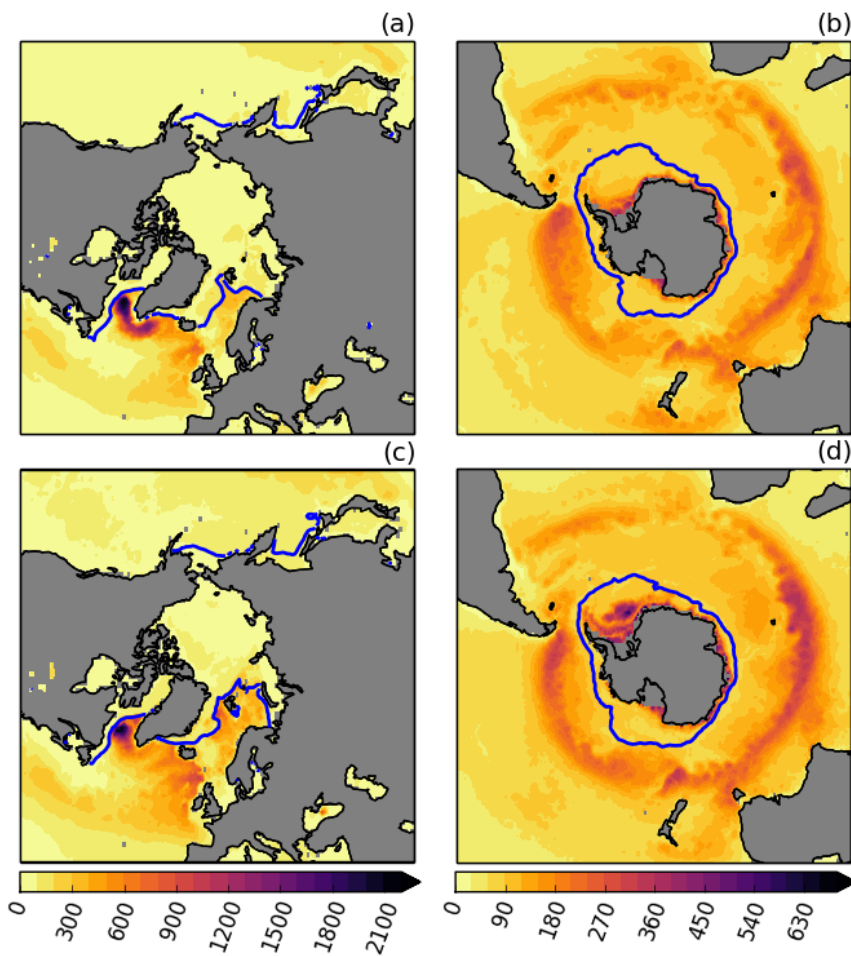


Formatted: No underline, Font color: Black

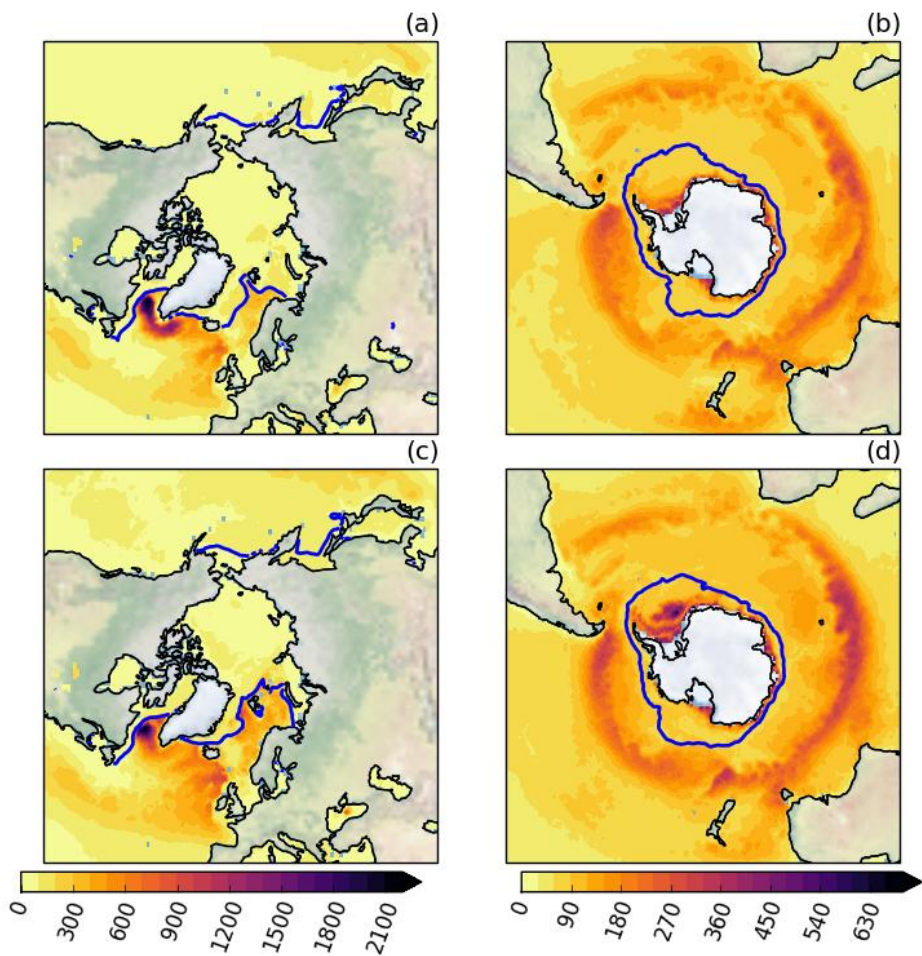
1



1
2
3 Figure 5: Seasonal cycle of sea ice extent in a) Northern and b) Southern hemisphere for years
4 11-20 compared against HadISST 1980-99 and with +/- 20% error bars denoted.
5

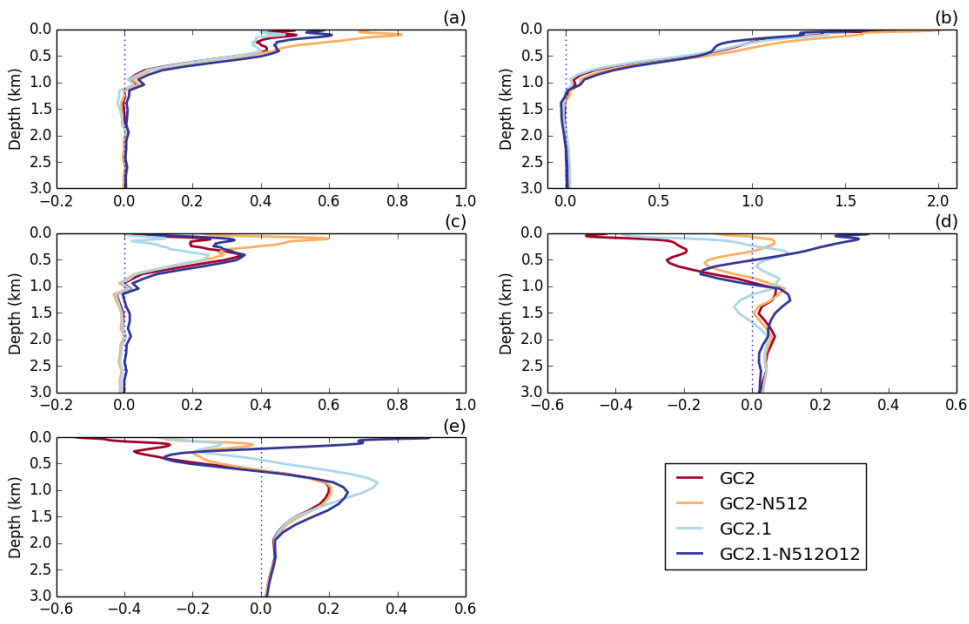


Formatted: No underline, Font color: Black

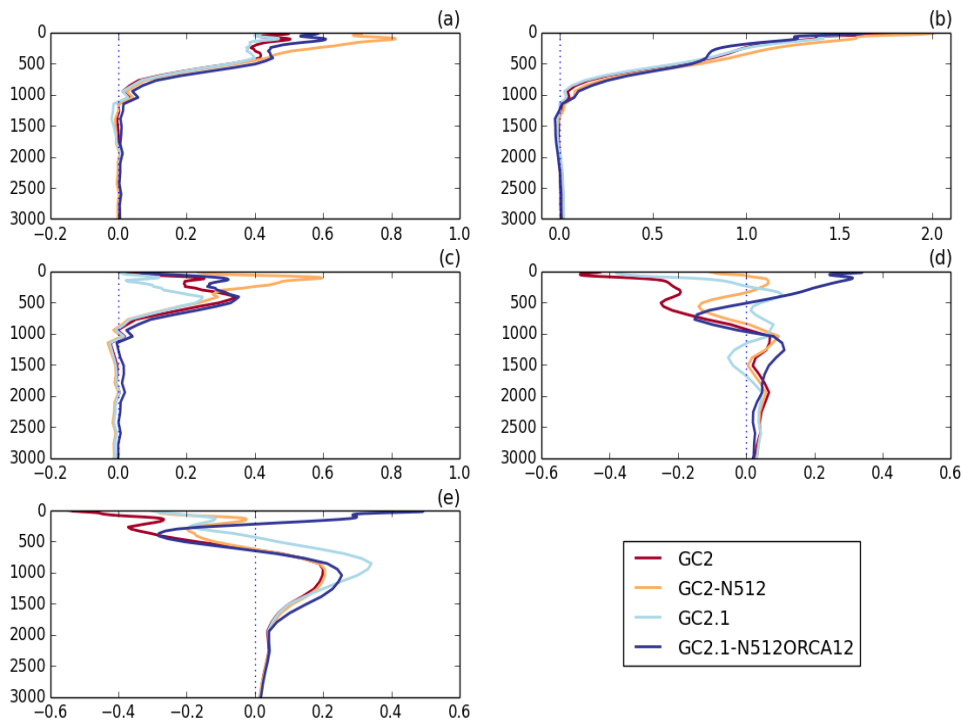


1
2
3
4
5
6
7
8

Figure 6: Mean March Northern hemisphere winter mixed layer depth (m) and Arctic sea ice edge and mean September Southern hemisphere winter mixed layer depth (m) and sea ice edge for years 11-20 for GC2 (a,b) and GC2.1-N512O12 (c,d). The sea ice edge (marked in blue) is based on a threshold of 15% ice concentration.



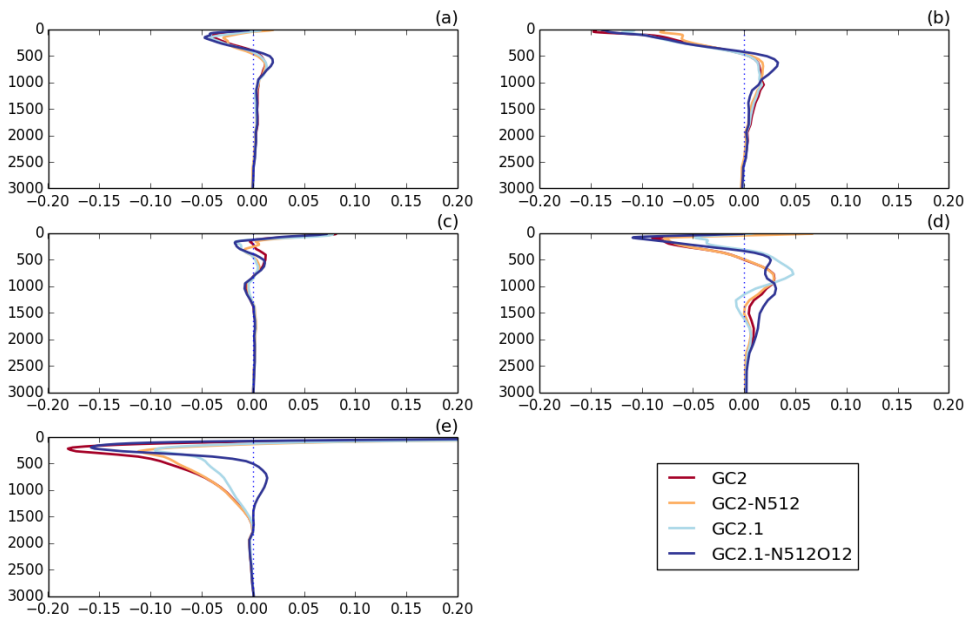
Formatted: No underline, Font color: Black

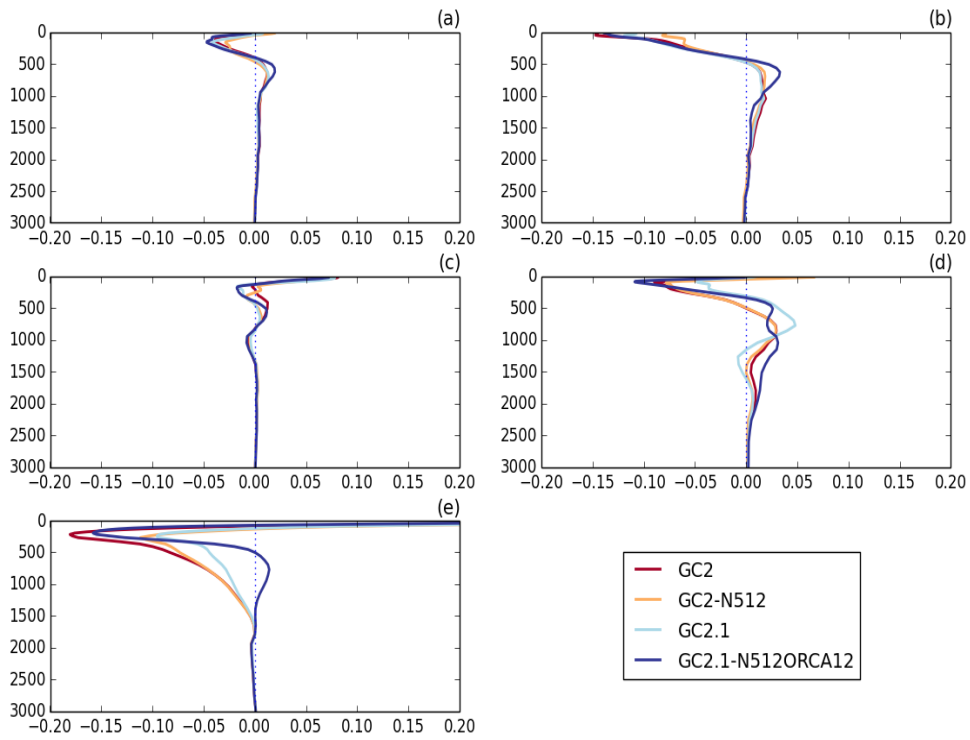


1
2
3
4
5
6
7
8

Figure 17: Area-weighted mean temperature difference (years 11-20 minus year 1; °C) for GC2, GC2-N512, GC2.1 and GC2.1-N512ORCA12 for a) global, b) 90S-30S, c) 30S-30N, d) 30N-90N, e) 65N-90N. Note the range on the x-axis is equal in all panels except (b). The vertical axis denotes depth (m).

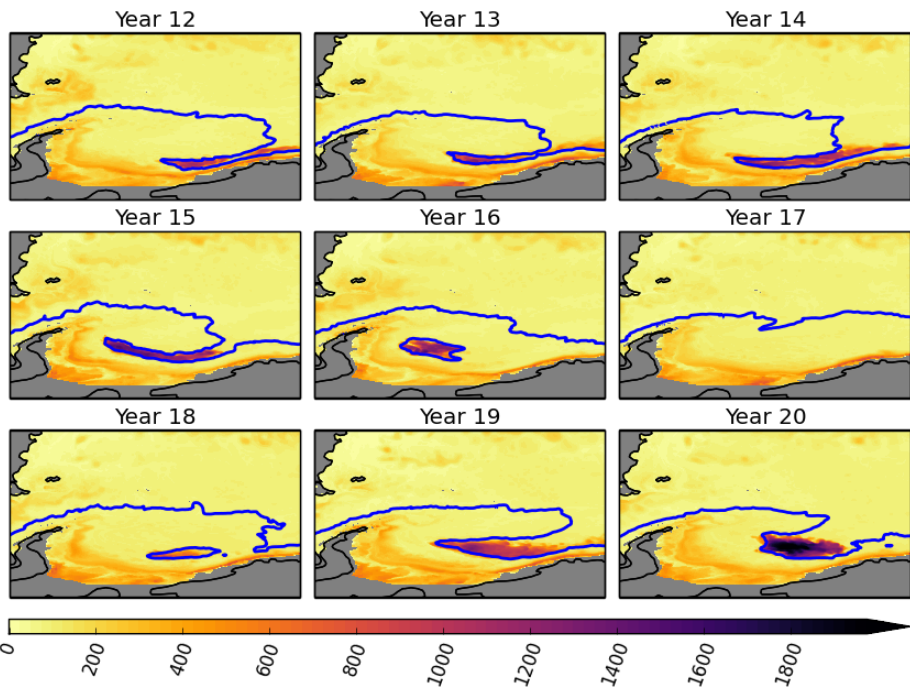
Formatted: No underline, Font color: Black





1 .
 2 Figure 88: Area-weighted mean salinity difference (years 11-20 minus year 1; psu) for GC2,
 3 GC2-N512, GC2.1 and GC2.1-N512O12 for a) global, b) 90S-30S, c) 30S-30N, d) 30N-90N,
 4 e) 65N-90N. The vertical axis denotes depth (m).

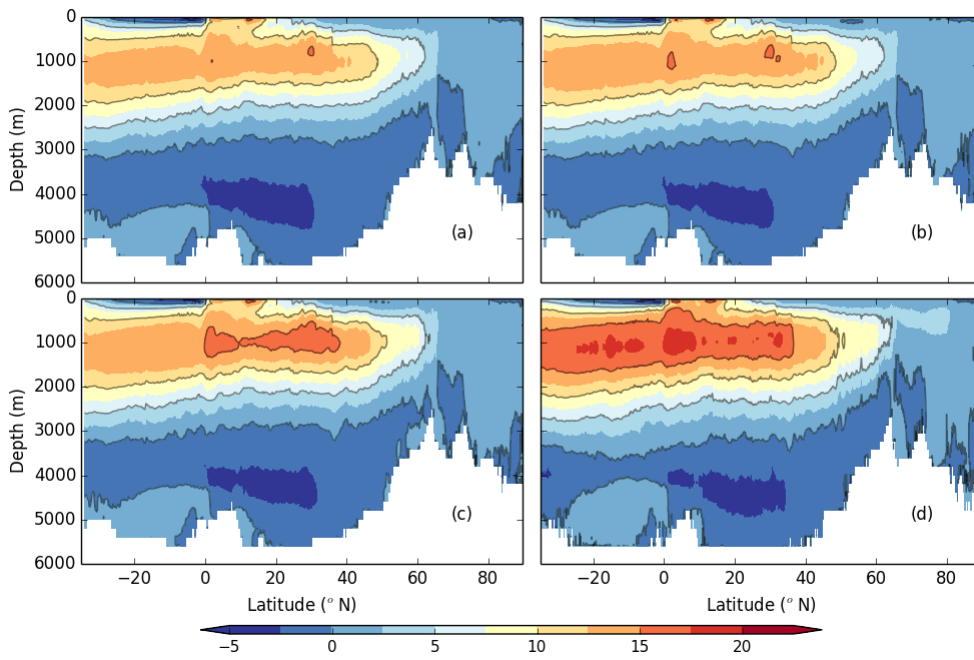
5
 6



Formatted: No underline, Font color: Black

1
2
3
4
5
6
7

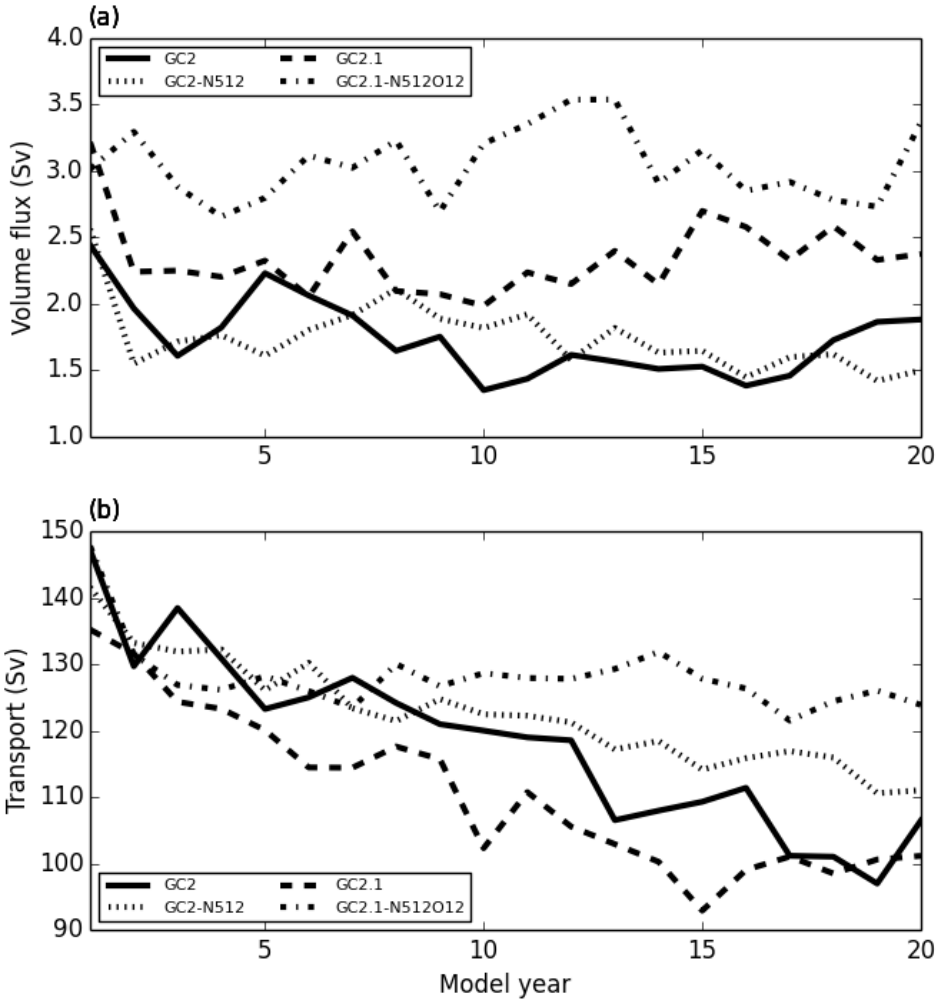
Figure 9: September mixed layer depth (m) and sea ice edge in GC2.1-N512O12 for years 12-20 indicating the presence of a Weddell Sea polynya. The sea ice edge (marked in blue) is based on a threshold of 15% ice concentration.

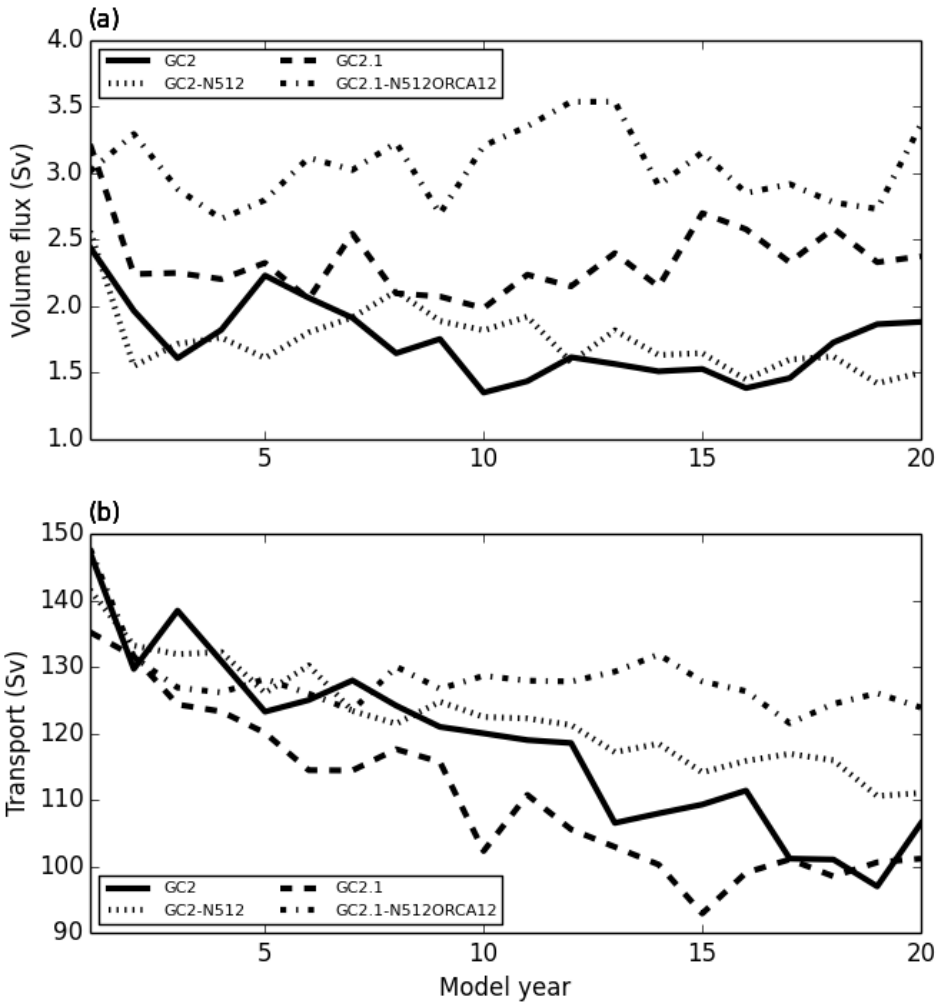


1
2
3 | Figure 109: Atlantic Meridional overturning for (a) GC2, (b) GC2-N512, (c) GC2.1 and (d)
4 | GC2.1-N512O12, meaned over years 11-20. Contours in Sverdrups ($10^6 \text{ m}^3\text{s}^{-1}$), with line
5 | contour spacing of 5 Sv.

6 |
7 |
8 |
9 |

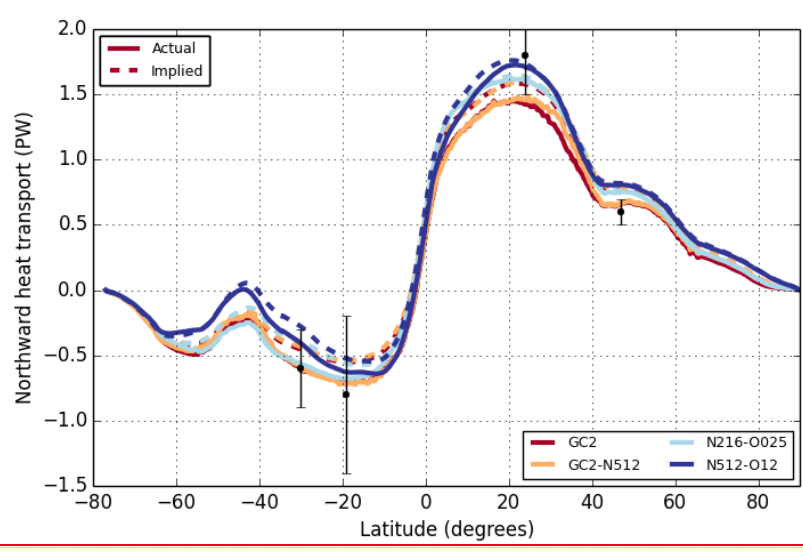
Formatted: No underline, Font color: Black



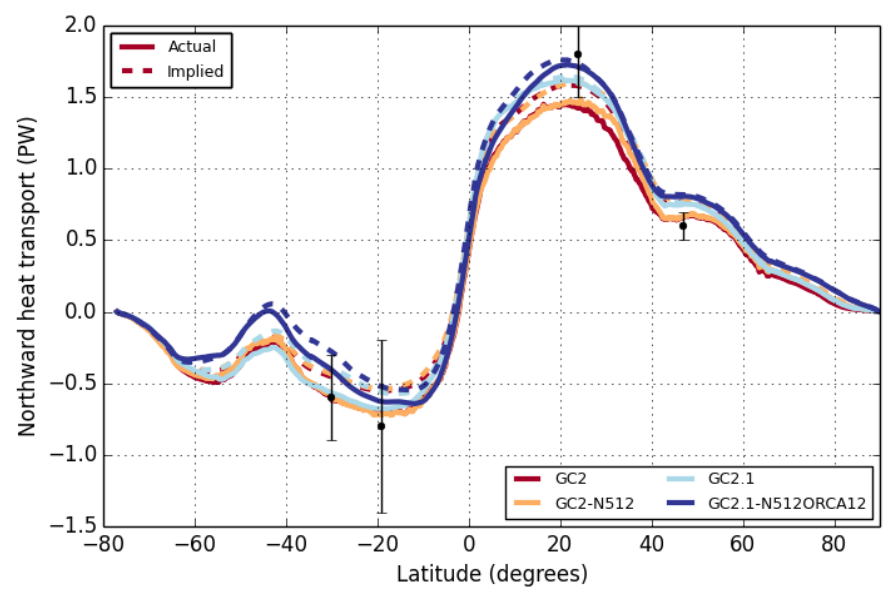


1
 2
 3 Figure 119: a) Denmark Straits volume flux (Sv) (calculated as southward flow across the
 4 Greenland-Iceland-Scotland ridge below density of 27.8 kg m^{-3}) and b) Antarctic Circumpolar
 5 Current transport (Sv) from GC2, GC2-N512, GC2.1 and GC2.1-N512O12
 6

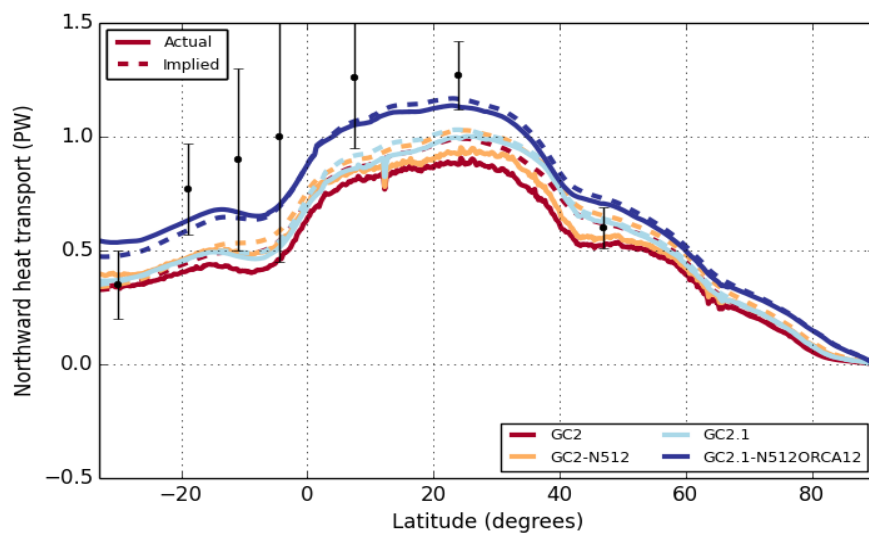
Formatted: No underline, Font color: Black



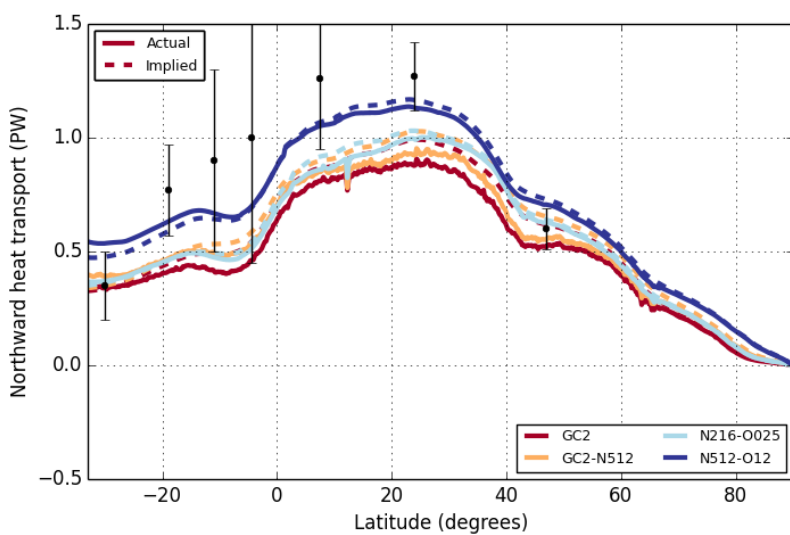
1



2



Formatted: No underline, Font color: Black



Formatted: No underline, Font color: Black

1

2

3 Figure 124: Actual (bold) and implied (dashed) northward heat transports from GC2, GC2-
 4 N512, GC2.1 and GC2.1-N512O12 for (a) global and (b) Atlantic basins. The implied
 5 transport (integrated southwards from the **North Pole** using the ocean surface heat flux)
 6 uses heat fluxes in which the global mean imbalance has been removed at every point.
 7 Observational estimates and associated error bars from Ganachaud and Wunsch (2003) are
 8 shown.